CHARGING SYSTEM OF THE BATTERY OF AN ELECTRIC VEHICLE

A

DISSERTATION

SUBMITTED IN PARTIAL FULFILLMENT OF THE REQUIREMENTS FOR THE AWARD OF THE DEGREE OF

MASTER OF TECHNOLOGY
IN
POWER SYSTEM
(2018-2020)

SUBMITTED BY:

APARNA LAL

2K18/PSY/01

UNDER THE SUPERVISION OF

PROF. MUKHTIAR SINGH

DEPARTMENT OF ELECTRICAL ENGINEERING
DELHI TECHNOLOGICAL UNIVERSITY

(Formerly Delhi College of Engineering) Bawana Road, Delhi-110042

AUGUST, 2020

\

DELHI TECHNOLOGICAL UNIVERSITY

(Formerly Delhi College of Engineering) Bawana Road,

Delhi-110042

CANDIDATE'S DECLARATION

I **APARNA LAL**, Roll No – **2k18/PSY/01** student of M.Tech (Power System), hereby declare that the project Dissertation titled "**CHARGING SYTEM OF THE BATTERY OF AN ELECTRIC VEHICLE**" which is submitted by me to the Department of Electrical Engineering, Delhi Technological University, Delhi in partial fulfilment of the requirement for the award of the degree of Master of Technology, is original and not copied from any source without proper citation. This work has not previously formed the basis for the award of any Degree, Diploma Associateship, Fellowship or other similar title or recognition.

Place: Delhi

Date:27-08-2020

(APARNA LAL)

ELECTRICAL ENGINEERING DEPARTMENT

DELHI TECHNOLOGICAL UNIVERSITY

(Formerly Delhi College of Engineering) Bawana Road, Delhi-110042

CERTIFICATE

I hereby certify that the Project Dissertation titled "**CHARGING SYTEM OF THE BATTERY OF AN ELECTRIC VEHICLE**" which is submitted by **APARNA LAL**, whose Roll No. is **2K18/PSY/01**, Electrical Engineering Department, Delhi Technological University, Delhi in partial fulfilment of the requirement for the award of the degree of Master of Technology, is a record of the project work carried out by the students under my supervision. To the best of my knowledge this work has not been submitted in part or full for any Degree or Diploma to this University or elsewhere.

Place: Delhi **PROF. MUKHTIAR SINGH**

Date: 29-08-2020 (**SUPERVISOR)**

ABSTRACT

This project presents the design and implementation of a single-phase on-board bidirectional plug-in electric vehicle (PEV) charger that can provide reactive power support to the utility grid in addition to charging the vehicle battery. The topology consists of two-stages: 1) a full-bridge ac–dc converter; and 2) a bidirectional dc–dc converter. It also implements a unified controller to follow utility PQ commands in a smart grid environment. The cascaded two-stage system controller receives active and reactive power commands from the grid, and results in line current and battery charging current references while also providing a stable dynamic response. The vehicle's battery is not affected during reactive power operation in any of the operation modes. The system described above, is performed in the same environment, using two different controllers. The first controller used is the convention PID controlling and the second one used is the model predictive controlling, which is quite in trend these days, owing to its predictability of the reference of the controlled variable for the next state. This ability of the predicting the desired behavior of the system in future, based on its behavior in present, helps the system to become more active, reacting fast to the change in controlling actions and also giving less deviation from the desired response within a reduced settling time.

Aug, 2020 **APARNA LAL**

Delhi (India) Roll No: **2K18/PSY/01**

ACKNOWLEDGEMENT

I would like to thank to all people who have helped and inspired me during my dissertation work throughout these years.

I sincerely acknowledge the earnestness and patronage of my guide **Prof. Mukhtiar Singh**, Department of Electrical Engineering, Delhi Technological University, New Delhi, for his valuable guidance, support and motivation throughout this project work. The valuable hours of discussion and suggestion that I had with him have undoubtedly helped in supplementing my thoughts in the right direction for attaining the desired objective.

I wish express my love and gratitude to my beloved parents, siblings and friends for their understanding and endless love. Above all, thanks to Almighty for blessing and guiding me throughout my life.

APARNA LAL

(2k18/PSY/01)

TABLE OF CONTENTS

PARTICULARS	PAGE NO.
CANDIDATE'S DECLARATION	ii
CERTIFICATE	iii
ABSTRACT	iv
ACKNOWLEDGEMENT	v
"TABLE OF CONTENTS"	vi
LIST OF FIGURES	viii
ACRONYMS	xiii
CHAPTER 1	1
INTRODUCTION	1
1.1: GENERAL	1
1.2: BATTERIES IN ELECTRIC VEHICLE	2
1.3: CHALLENGES TO THE ELECTRIC VEHICLE: BATTERY	3
1.4: CHARGING POWER LEVELS	4
1.5: ON-BOARD AND OFF-BOARD CHARGERS	5
1.6: UNI-DIRECTIONAL AND BI-DIRECTIONAL CHARGERS IN EVs	7
Unidirectional Chargers	7
Bi-directional Chargers	8
1.7: WHAT IS CONDUCTIVE CHARGING ?	8
1.8: INDUCTIVE CHARGING	9
1.9: CHALLENGES, TRENDS AND EFFECTS	9
1.10: COMPONENTS OF THE BATTERY CHARGING	11
1.11: THE AC TO DC CONVERSION	12
1.12: THE DC TO DC CONVERSION	12
CHAPTER 2	
LITERATURE REVIEW	14
2.1: TRANSFORMATION	14
2.2. MATHEMATICAL MODEL OF A RECTIFIER	17
2.3. MATHEMATICAL MODELLING OF A CHOPPER	18
2.4. DQ TO ALPHA-BETA CONVERSION	20

2.5. SECOND ORDER GENERALIZED INTEGRATOR (SOGI) 21
2.6. PHASE LOCKED LOOP (PLL) 21
CHAPTER 3
THE CONTROLLING STRATEGIES 23
3.1: INTRODUCTION 23
3.2. THE PID CONTROLLING 26
3.2.1: Methodology 27
3.3 THE MODEL PREDICTIVE CONTROL 30
3.3.1: Methodology 32
3.3.2 Optimisation of Cost Function 35
CHAPTER 4 42
SIMULATION AND RESULTS 42
4.1 PARAMETERS 42
4.2 THE PI CONTROLLED SYSTEM 43
4.3 THE MODEL PREDICTIVE CONTROLLED SYSTEM 45
CONCLUSION AND FUTURE SCOPE 50
REFERENCES 51

LIST OF FIGURES

Figure 1: Electric Vehicle……2
Figure 2: On-board and Off-board Charging……5
Figure 3: Types of DC to DC converters 13
Figure 4: Rectifier Topology 14
Figure 5: Reference Frame of abc and alpha-beta system 15
Figure 6: dq and αβ frame of reference 16
Figure 7: Modelling of Rectifier 17
Figure 8: Buck converter 18
Figure 9: Buck converter operation with switch closed 18
Figure 10 : Buck converter operation with switch open 19
Figure 11: Converter Control Methods 23
Figure 12: Outline of the system control via PID controller 27
Figure 13: Block diagram of complete PI controlled system 29
Figure 14: General MPC scheme 31
Figure 15: Block Diagram of MPC controlled system 32
Figure 16: The single phase rectifier 32
Figure 17:Block diagram of MPC controlled single phase rectifier 38
Figure 18: Block diagram of the MPC controlled DC to DC converter 38
Figure 19: Block diagram of the PID controlled charging system 43
Figure 20: Rectifier controller……43
Figure 21: Simulation model of PID controller charger system……44
Figure 22: Active power control comparison……44
Figure 23: Reactive power control comparison……44
Figure 24: PI control of the battery current……45
Figure 25: Battery performance……..46
Figure 26: Block diagram of MPC control charging system……...46
Figure 27: Alpha-beta components of the source voltage using SOGI……..46
Figure 28: Alpha-beta components of the source current using SOGI……..46
Figure 29: Comparison of active power controlled with reference power generated…47

Figure 29: Comparison of reactive power controlled with reference power generated…….48
Figure 30: MPC controlled inductor current comparison……...48
Figure 31: MPC controlled battery characteristics…….49

LIST OF TABLES

Table 1: Levels of charging…….....4
Table 2: Comparison of On-board and Off-board charging……6
Table 3: Properties of PID controller……27
Table 4: Converter parameters……..28
Table 5: Battery parameters……29

LIST OF SYMBOLS

α	**alpha-component**
β	**beta-component**
R	**source resistance**
L	**source inductance**
Ω	**ohm**
∅	**phi**
$\Re$	**vector**
$\Re_{\alpha}$	**alpha-component of the vector**
$\Re_{dq}$	**dq-component of the vector**
θ	**theta**
$\Re_{d}$	**direct-component of the vector**
$\Re_{q}$	**quadrature-component of the vector**
i_{α}	**alpha-component of source current**
i_{β}	**beta-component of source current**
u_m	**sdfgh**
E_m	**maximum amplitude of voltage**
I_m	**maximum amplitude of current**
u_s	**supply voltage**
u_b	**voltage of point 'b'**
u_{dc}	**dc voltage**
i_{load}	**load current**
$u_{s\alpha}$	**alpha-component of supply voltage**
$u_{s\beta}$	**beta-component of supply voltage**
$u_{b\alpha}$	**alpha-component of voltage u_b**
$u_{b\beta}$	**beta-component of the voltage u_b**
V_O	**output voltage**
V_S	**supply voltage**
i_L	**inductor current**
i_o	**output current**
i_C	**capacitor current**

V_c	capacitor voltage
K_P	proportional constant
K_I	integral constant
K_D	derivative constant
S	apparent power
V_{sm}	maximum amplitude of supply voltage
m_F	modulation function
T_s	sampling time
I_{ref}	reference current
V_{ref}	reference voltage

ACRONYMS

EV	Electric Vehicle
HEV	Hybrid Electric Vehicle
SoC	State of Charge
PFC	Power Factor Correction
SOGI	Second Order Generalized Integrator
PLL	Phase Locked Loop
PID	Proportional Integral Derivative
DTC	Direct Torque Control
DPC	Direct Power Control
FOC	Flux Oriented Control
VOC	Voltage Oriented Control
MPC	Model Predictive Control
GPC	Generalized Predictive Control
IGBT	Insulate Gate Bi-polar Transistor
SMC	Sliding Mode Control
MOSFET	Metal Oxide Silicon Field Effect Transistor
PWM	Pulse Width Modulation
SLI	Starting Lightening Ignition
EVSE	Electric Vehicle Supply Equipment
BMS	Battery Management System

CHAPTER 1

INTRODUCTION

1.1: GENERAL

A multitude of vehicles using fossil fuel usage is increasing with the rising living standards. These carbon-fuel dependent vehicles are emitting carbon dioxide which is hitting a record high in the current year, increasing at the rate of 2.6 percent per annum. Though, each region is grappling in its own unique way, one of the ways, to address the upsurge in emission and increased pollution, is by increasing the use of electric vehicles.

An electric vehicle maneuvers one or more electric motors for propulsion. It may be powered through a converter system by electricity from off vehicle sources or may be self-contained with a battery or a generator to convert fuel to electricity[51]. EVs vary from road to rail vehicles, surface to underwater vehicles, electric aircraft to spacecrafts.

Characteristics of an EV:

- **Powered By Electricity:** Gas tank is not required, electric vehicles are powered by batteries which get energy from electricity
- **Inverter/Charger:** AC to DC (Off-board) and DC to DC (On-board)
- **Traction Battery:** Gradually run down as the EV drives, required DC voltage to charge
- **Electric Motor:** Drives the gearbox and wheels, not an engine. Electric energy is fed into the coil to induce a magnetic field making the coil rotate very quickly inside the magnets. Spinning coil is fastened to the central shaft that drives the wheels.

An EV can be classified into:

- Electric vehicle

- Hybrid Electric vehicle
- Plug-in Hybrid Electric vehicle

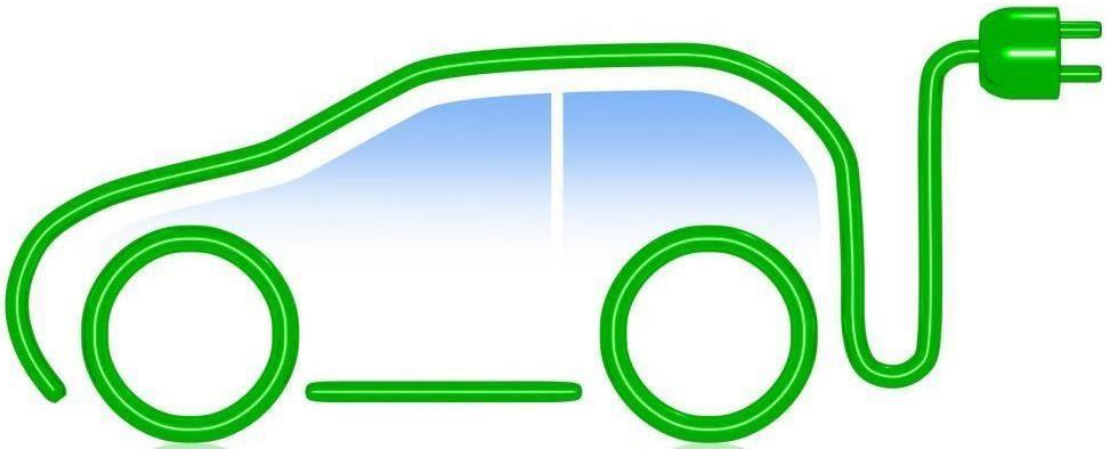

Fig. 1: Electric Vehicle

1.2 BATTERIES IN ELECTRIC VEHICLE

Battery is one of the important components that decides the performance of EV. It consists of electrochemical cells with it's external connections provided to give power to the vehicle. The development of the technology of the battery for EVs started from the early use of lead-acid batteries in the late nineteenth century to the lithium-ion batteries the 2010s, which are found in most EVs today. A battery pack overall is a group of multiple battery modules and battery cells. The battery pack used for powering electric vehicles can use as little as 96 battery cells to as many as 2,976 cells. There are two kinds: primary and secondary. Here, vehicle batteries are usually a rechargeable secondary battery. Electric golf carts, electric cars, trucks, vans, EVs, electric forklifts, golf carts, etc use the traction batteries. One of the categories of the battery is an SLI battery, which stands for starting, ignition and lighting [52]. SLI battery is a rechargeable type lead-acid battery which is conventionally used in the automobiles. Another type is the deep cycle batteries in which the discharge of the battery is very deep compared to that of the. Electricity charged battery vehicles differ from starting, lighting, and ignition (SLI) vehicles because they are designed to give power over sustained periods of time [52]. Deep cycle batteries are used instead of SLI batteries for these applications. Designing of the traction batteries are done with a high ampere-hour capacity perspective. Batteries for electric vehicles are characterized by [52]:

- high power-to-weight ratio
- specific energy and energy density
- smaller size

Lighter batteries provide an advantage of reduced body weight of the vehicle and improved performance. Most of the current battery technologies, in comparison to the liquid fuels, have much lower specific energy, which impacts the maximal all-electric range of the vehicles. Although, the specific energy is high for the metal-air batteries due to the cathode provided, being surrounded by the oxygen in the air. Nickel-metal hydride, nickel-cadmium, lithium-ion, lead-acid, lithium-ion polymer, zinc-air are few of the types of batteries used in the rechargeable batteries of electric vehicles. The most common battery type in modern electric cars is lithium-ion and lithium polymer battery, because of their high energy density compared to their weight [52]. Ampere-hours and coulombs are the units used to express the amount of electrical energy stored in the batteries in the form of charge. Ampere-hours is the preferred unit. Also, the total energy of the battery can be measured in watt-hours.

1.3 CHALLENGES TO THE ELECTRIC VEHICLE: BATTERY CHARGING

The main reason for the slow acceptance of the EVs is mainly due to its battery performance. The challenges faced by EV batteries mainly consist of:

- high cost
- cycle life of batteries
- complications of chargers
- the lack of charging infrastructure

Another drawback is that battery chargers can produce deleterious harmonic effects on electric utility distribution systems, although chargers with an active rectifier front end can mitigate this imp.

1.4 CHARGING POWER LEVELS

Charger power levels reflect power, charging time and location, cost, equipment, and effect on the grid [1]. The electric-vehicle-supply-equipment (EVSE) and the charging stations deployed is a very important step because of many issues that need to be addressed which includes demand, extent, distribution, policies framed to meet those demands, standardization of charging-station[1] and regulatory procedures [1]. Most of the time, customers prefer to charge EV at their own dispense i.e., it will be very convenient for them if the charging can take place overnight at their home in a garage where you can plug the EV into a convenient outlet [2]. There are three levels of charging:

	Voltage Level	Charging Time
Level 1	120 V	16-20 hrs
Level 2	240 V	6 hrs
Level 3	480 V	< 1 hr

Table 1. : Levels of charging

Level 1: It is the slowest method. It uses standard 120V/ 15A single phase grounded outlet [1] in US. It can add about 40 miles of range in an eight-hour overnight charge. Overnight Level 1 charging is suitable for low- and medium-range plug-in hybrids and for all-electric battery electric vehicle drivers with low daily driving usage.

Level 2: Stations for public use are likely to use level 2 charging. The existing level 2 equipment offers charging from 208V or 240V [1]. It may require dedicated equipment and a connection installation for home or public units, although vehicles such as the Tesla have the power electronics on board and need only the outlet. Level 2 devices can charge a typical EV battery overnight [2]. The new standard has an SAE J1772 [65] ac charge connector on top and a two-pin dc connector below and is intended to enable either ac or dc fast charging via a single connection.

Level 3: Level 3 commercial fast charging offers the possibility of charging in less than 1 h [1]. It can be installed in highway rest areas and city re-fuelling points, analogous to gas stations [1]. It typically operates with a 480 V or higher three-phase circuit and

requires an off-board charger to provide regulated ac–dc conversion[1]. The connection to the vehicle may be direct dc. Level 3 charging is rarely feasible for residential areas [1]. A lower charge power is an advantage for utilities seeking to minimize on-peak impact. High power rapid charging can increase demand and has the potential to quickly overload local distribution equipment at peak times. Level 2 and 3 charging can increase distribution transformer losses, voltage deviations, harmonic distortion, peak demand, and thermal loading on the distribution system. This could significantly impact transformer life, reliability, security efficiency, and economy of developing smart grids due to reduced transformer life [1].

1.5 ON BOARD AND OFF-BOARD CHARGERS

Similar to the manner in which the location, size and energy density of the battery affects the performance of the vehicle, the location and size of the charger, if present inside the vehicle, affects the performance of it. Based on the location at which the charger is present, the chargers can be classified mainly into two categories:

1. On-Board Charger [53]
2. Off-Board Charger [53]

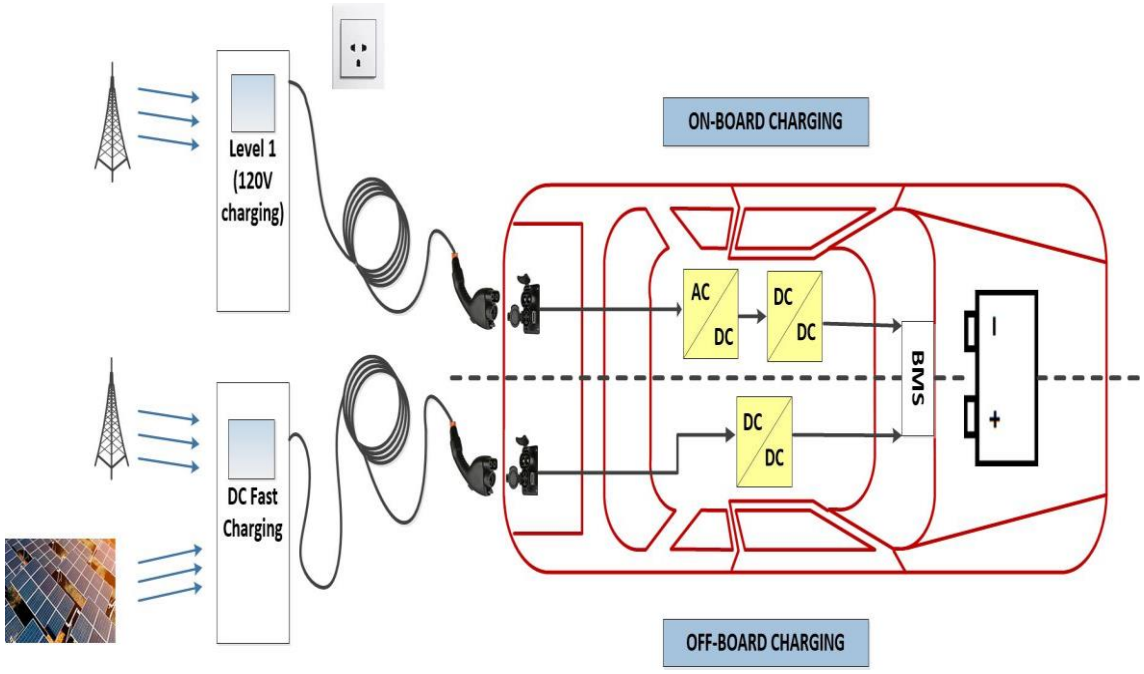

Fig. 2 : On-board and Off-board Charging

	ON-BOARD CHARGER	OFF-BOARD CHARGER
1. Location	Inside vehicle	Outside vehicle
2. Charging feasibility	Allows charging wherever feasible power source is available	Possible only at the charging stations
3. Kilowatt transfer	Higher kilowatt transfer is possible	Relatively less kilowatt transfer
4. Level	Limits the power to level 1[1]	Allows level 2 and level 3 power transfer limit [1]
5. Redundancy	Less redundant use of power electronic	More redundancy
6. Vandalism	Minimum risk of vandalism	Increased risk of vandalism
7. BMS	Less sophisticated BMS works for on-board charger	A sophisticated battery management system is required
8. Space constraint	Less space constraint	More space constraint
9. Cost constraint	Cost is comparatively less	Cost is more
10. Weight	Weight added to the vehicle due to charger topology is comparatively more.	Weight added to the vehicle is comparatively less because.
11. Space constraint	No. of power electronics components per unit area is more.	Space constraint is comparatively less.
12. Cooling system	Because of low level of power transfer, heating is relatively low.	Charger gets heated up quickly and requires efficient cooling system.
13. Energy transfer rate	Low	High
14. Waste generation	Adds less clutter.	Adds more clutter to the environment.

Table 2: Comparison of ON-board and Off-board charger

1.6 UNIDIRECTIONAL AND BIDIRECTIONAL CHARGERS EVs

Energy flow in the EVs takes place between the grid and the battery through the converter system. This rush of energy is determined by the kind of switches used in the converter system. The switches that can be used ranges from simple diode to BJT, MOSFET, IGBT, thyristors, DIAC, TRIAC, etc. BJT, thyristor, diode are all unidirectional in nature i.e. they permit the circulation of current in the positive direction only. Whereas, MOSFET and IGBTs are bidirectional devices i.e. current can pass in either direction via them. Similarly, electric vehicles are also categorized based on the direction of flow of energy in the system:

1. Uni-directional charger
2. Bi-directional charger

Uni-Directional Charger : Uni-directional chargers can charge the EV battery but it cannot inject energy back into the power grid. As asserted before, it uses the switches that permits the flow of current only in the forward direction. Thus, it can use uni-directional switches such as diode, BJTs, thyristors, etc. In conjunction with the switches utilised for the AC to DC conversion, a filter and a DC to DC converter is also used here. Application of these converter in a single stage is desired so that volume, weight, power density, cost and losses can be limited.

Use of high-frequency isolation transformers is also in demand and it is employed when reduction in loss, improvement in efficiency, low level of switching losses, etc is desired which is a result of high frequency. The controlling topology of the uni-directional system is comparatively easier than that of the bidirectional chargers. This simplicity makes it easier for implementation, which can manage heavily loaded feeders connected to a number of electric vehicles charging at the same time. Those with active front ends can provide local reactive power support by means of current phase angle control without having to discharge a battery. It achieves objective of cost avoidance, performance and safety concerns which is also associated with bidirectional chargers. These chargers can use non-isolated or isolated circuit layouts[1]. When operating in charge mode, they should draw a sinusoidal current with a defined phase angle to control power and reactive power [1]. In discharge mode, the charger should remit current back in a similar sinusoidal form [1].

Bi-directional Charger : A bidirectional charger supports charge from the grid, battery energy injection back to the grid, referred to as vehicle-to-grid (V2G) operation mode, and power stabilization [54]. Bidirectional chargers are expected only for Level 2 infrastructures, because Level 1 power limits and cost targets are low, and it is vital to maximize flexibility. In Level 3 fast charging, reverse power flow conflicts with the basic purpose and premise of minimizing connection time and delivering substantial energy as quickly as possible [1].

At the beginning and end of the day, the electric vehicles are used as a medium of transport. On arriving at the destination, electric vehicles are plugged into charge. This is the time when the electricity grid is most under pressure due to spike in demand a sudden spike sometimes a backup power is used as a lending hand. But instead of taking energy from the grid it would be great if the electric vehicle could support the system. If the charge is still left in the vehicle then it can be used for the purpose of driving the appliances of home in any residential area. There are two electric vehicles can be used to power a household or it can be used to export the power back to the grid during peak hours and during off peak hours the great can be used to charge the battery of the electric vehicle. This can be used to provide incentive to the customers that is as a way of earning for the customer. It can also be used in order to bring an environment of a reliable sustainable and more affordable energy

1.7 WHAT IS CONDUCTIVE CHARGING?

Conductive charging uses metal-to-metal contact as present in most appliances and electronic devices. Conductive charging is a method that requires a physical connection to be made between the portable device's battery and the charging station. Special attachments are made that are fitted to the electronic device, making it compatible with the charging base. The wireless charging base is able to detect when a compatible device has been placed on it, and passes an electrical current from the base to the electronic device through the special attachments The cable can be fed from a standard electrical outlet (Level 1 or 2) or a charging station (Level 2 or 3) [1]. There are already several charging posts on the market [1]. Available vehicles, including the Chevrolet Volt and Tesla Roadster, use Levels 1 and 2 chargers with basic infrastructure (convenience outlets) [1]. Conductive charging is also employed on the Nissan Leaf and Mitsubishi i-MiEV, which use either basic infrastructure or dedicated off-board

chargers [1]. The main drawback of this solution is that the driver needs to plug in the cable. This is a conventional issue [1].

1.8 INDUCTIVE CHARGING

Inductive charging is based on magnetic contactless power transfer. This type of charger has been explored for Levels 1 and 2 devices. The clear advantage of contactless charging is its convenience for the user. Instead of deep-cycling the battery, the vehicle battery can be topped off frequently while parked at home or at work, when shopping and even at traffic lights. Cables and cords are eliminated. Advantages include convenience and galvanic isolation. It is also possible to build charging strips into highways which enables charging while driving. Therefore, inductive charging could strongly reduce the need for a fast-charging infrastructure. Disadvantages include relatively low efficiency and power density, manufacturing complexity, size, and cost. Given that energy savings is an important motivator for EVs, the extra power loss is an important consideration [1].

1.9 CHALLENGES, TRENDS AND EFFECTS

Barriers to infrastructure installations are:

1. Installation costs
2. Utility infrastructure planning and construction
3. Consumer knowledge
4. Metering, contractor role, permitting procedures, etc [55].

The demand for charging infrastructure is driven by three main factors:

- penetration rates
- degree of charging
- range anxiety [55]

Challenges include:

- Uncertainty regarding the impact of the smart grid on EV batteries and charging

infrastructure [55].

- Levels I and II slow charging will likely be the most used schemes because of convenience and low-cost electricity. Home charging will be important for achieving high rates of EV deployment; public charging is arguably more important for moving past the very early stages of EV adoption. This infrastructure is the most economical because it does not require a wall box. However, as battery capacity and range of EVs are improved, and potentially some EVs in the future would need Level III fast charging to extend the driving range, there is an increased need to build off-board charge station infrastructures. Level III fast charging provides a method to alleviate range anxiety for the driver of passenger EVs [55].

- The high cost of installing a rapid-charging infrastructure

- Constraint on storage of batteries and inductive charging

- The difficulty associated withdrawing large amounts of energy from the electricity grid ensure that overnight and standard charging will remain. The most common methods for vehicle charging [1]. The need for recharging in the community and on highways—preferably fast charging—is essential for mass commercialization [1].

The successful deployment of EVs over the next decade is dependent on the following:

1) deploying a charging infrastructure and associated EVSE is perhaps the most important consideration. Necessary parts include conductors, EV connectors, attachment plugs, devices, power outlets, or other apparatus installed specifically for the purpose of safely delivering energy from the premises wiring to the EVs;

2) charger reliability, durability, and safety considerations will contribute to consumer acceptance of EVs [55];

3) charger efficiency and reducing charger costs [55];

4) suitability for V2G-bidirectionalpowerflow,communication, and metering [55];

5) charging systems that can accommodate high-power charging will provide more flexibility and choices to the consumer [55];

6) charging strategies and setting limits for charging time and access rules;

7) the introduction of internationally agreed upon EV standardization of charging stations [55].

The parameter on which the use of electric vehicles is analyzed is dependent on state of charge (SoC), time of charging, ampere-hour rating, voltage and current control in a battery.

There are different levels of charging available: level 1, level 2 and level 3. Among these, level 1 charging allows the charging of the battery from a source of 120 volts and is the most commonly, to-be-used level of charging since it is easily available at the dispense of the customer.

The world transportation energy usage is going to increase by up to 44% by year 2035 (compared with 2008). With depleting fossil fuel reserves and increasing urban air pollution (particulate matter, ozone and smog formation, and greenhouse gases), transportation oil consumption needs to be more effectively regulated, and alternative vehicle technologies should be developed. Plug-in electric vehicles (PEVs) rely on electric traction power, which is more efficient. A PEV can save more than $700 annually on fuel consumption compared with internal combustion engine vehicles due to more energy efficient operation. Off-board fast charging stations are a key factor for the widespread market penetration of PEVs. Off-board chargers extend the time/miles that a vehicle is used with battery power and help customers overcome the range anxiety for PEVs. With advancing battery technologies, it is becoming possible to charge vehicle batteries at higher power levels. Therefore, at present, off-board fast charging solutions are offered to expedite the charging process. At these charging stations, ac voltage is converted into dc off the vehicle, and the vehicle is dc coupled to the charging station. Currently, there are several off-boards fast charging station coupling standards, such as Chademo and combined charging systems. The standards support up to a dc charging of 50 kW at voltages ranging between 100 and 600 V in order to meet different dc battery voltage levels.

1.10 COMPONENTS OF BATTERY CHARGING:

The main objective here is to design:

1. AC to DC converter
2. DC to DC converter
3. PFC (power factor correction block)

1.11: THE AC TO DC CONVERSION

This is the first stage in the charging of the battery of an electric vehicle. The conversion from AC to DC is done with the help of converters, also known as rectifiers. The source of the converters could be three phase AC or single phase AC, depending upon the level of charging and functions of the charger. In three phase rectification, the available converters vary from three phase Diode Bridge to fully controlled thyristor bridge to the full bridge converter cascaded with a switch in parallel and a diode in series to give a controlled and rectified output with a boost converter characteristic. The three phase converters also include a special topology of converter known as Vienna converter which has the advantage of simplicity, low switching losses and simple control.

The desired characteristic of a rectifier includes:

- better voltage regulation
- improved power factor
- low harmonic distortion of line current
- controlled power flow i.e. unidirectional and bidirectional

1.12: THE DC TO DC CONVERSION

The dc to dc converters are used to step up or step down the voltage source to a desired level of dc voltage. The most basic types of choppers include buck, boost, buck-boost converters with inverting and non-inverting topologies [4]. These converters are classified as isolated and non-isolated converters [4]. According to the configuration of converter topologies isolated converters have two configurations full and half bridge topologies [3]. In addition, the half-bridge converter needs a centre-tapped transformer, which results in a complex structure, and the full-bridge converters are required a higher number of semiconductor devices and cost of the converter also increased. In order to reduce the voltage stress caused by the leakage inductance, a DC-DC converter with an

active clamp circuit is used [3]. The leakage inductance utilized in dual active bridge and the phase-shift full-bridge to achieve the soft-switching, and stored energies in leakage inductance are transmitted to the load [4].

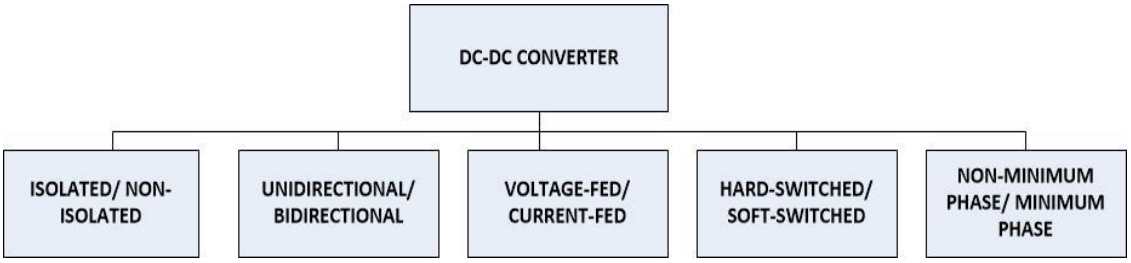

Fig. 3: Types of DC to DC converters

CHAPTER 2

LITERATURE REVIEW

2.1: TRANSFORMATION

Consider a single phase system with semiconductor switches to be connected in single phase full bridge configuration.

Assume semiconductor valves to be ideal.

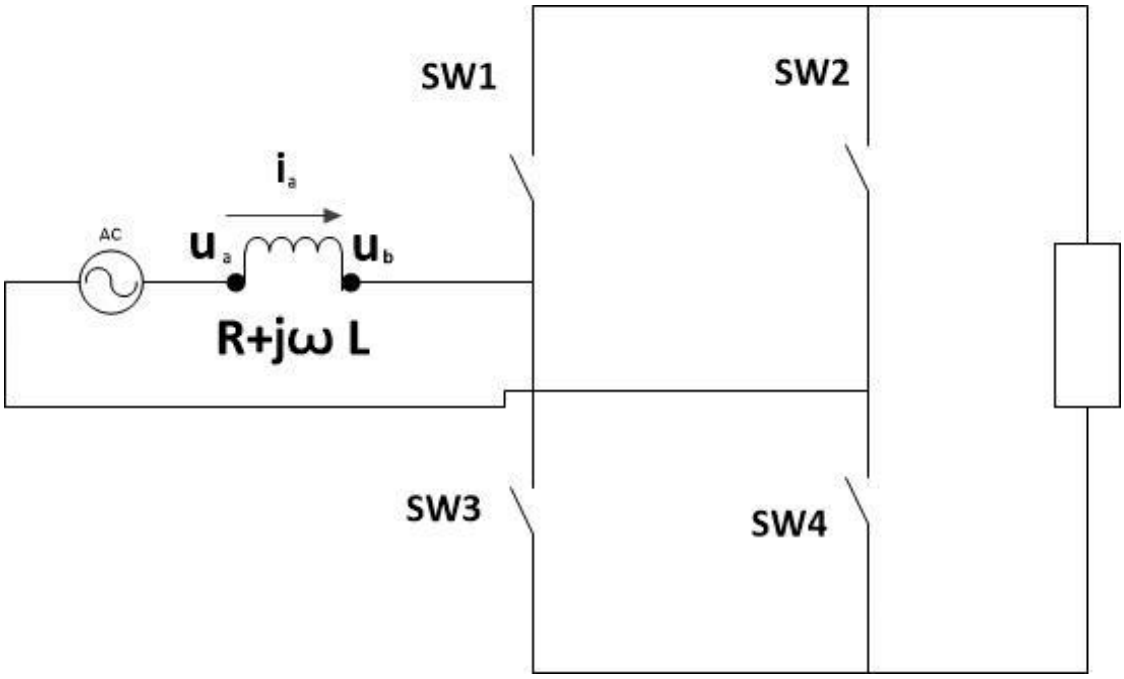

Fig. 4: Rectifier Topology

Here, consider voltage source to be defined as:

$$\mathbf{u_m(t) = E_m cos\ (\omega t)} \qquad \textbf{(2.1)}$$

Here, we can define current as:

$$\mathbf{i = I_m cos\ (\omega t + \emptyset)} \qquad \textbf{(2.2)}$$

Now, $\mathbf{u_s = u_a}$

By KVL at the source end, we get:

$$\mathbf{u_s = i(t)R + L\frac{di(t)}{dt} + u_b} \qquad \textbf{(2.3)}$$

By KCL at the load end:

$$\mathbf{C\frac{du_{dc}}{dt} = i(t) - i_{load}} \qquad \textbf{(2.4)}$$

Now, we try to synchronize the single phase ac system to the positive sequence part of the voltage of the source. Here, the purpose of conversion from AC to the other frame of reference is to decouple the controlling from a continuously rotating frame to a stationary $\alpha\beta$ frame and then to a synchronously rotating frame i.e. dq frame, which thereby, makes controlling easy.

Now we can't directly convert single phase AC to directly dq-system. Thus we use an indirect approach, by converting, single phase AC to $\alpha\beta$-system and thereby convert from $\alpha\beta$-system to dq-system.

Here, $\alpha\beta$-system is an orthogonal system, where alpha axis is aligned along the a-axis of the abc reference frame.

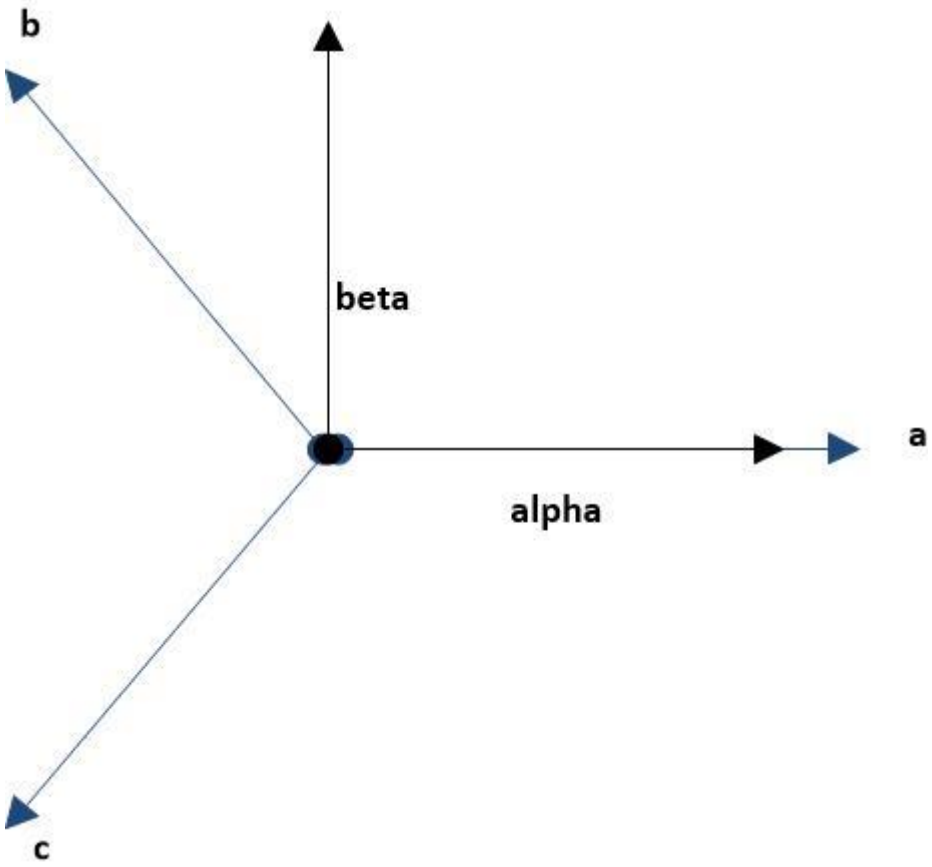

Fig. 5: Reference frame of abc and alpha-beta system

This transformation is also called as Clarke's transformation. Now, when we express a vector from abc system to alpha-beta system, we get a resultant vector in alpha beta system as:

$$\mathfrak{R} = r_a e^{j0} + r_b e^{j\frac{2\pi}{3}} + r_c e^{j\frac{4\pi}{3}} \quad \textbf{(2.5)}$$

$$\Rightarrow \mathfrak{R} = [r_a + r_b cos\left(\frac{2\pi}{3}\right) + r_c cos\left(\frac{4\pi}{3}\right)] + j[r_b sin\left(\frac{2\pi}{3}\right) + r_c sin\left(\frac{4\pi}{3}\right)]$$

$$\Rightarrow \mathfrak{R} = [r_a - 0.5r_b - 0.5r_c] + j[r_b\left(\frac{\sqrt{3}}{2}\right) - r_c\left(\frac{\sqrt{3}}{2}\right)]$$

$$\Rightarrow \mathfrak{R}_\alpha + j\mathfrak{R}_\beta = [r_a - 0.5r_b - 0.5r_c] + j[r_b\left(\frac{\sqrt{3}}{2}\right) - r_c\left(\frac{\sqrt{3}}{2}\right)]$$

We get a matrix in the form as shown below:

$$\Rightarrow \begin{bmatrix}\mathfrak{R}_\alpha \\ \mathfrak{R}_\beta\end{bmatrix} = \begin{bmatrix}1 & -\frac{1}{2} & -\frac{1}{2} \\ 0 & \frac{\sqrt{3}}{2} & -\frac{\sqrt{3}}{2}\end{bmatrix}\begin{bmatrix}r_a \\ r_b \\ r_c\end{bmatrix} \quad \textbf{(2.6)}$$

Now, applying the transformation to the equation (2.3), we get:

$$\begin{bmatrix}u_{s\alpha} \\ u_{s\beta}\end{bmatrix} = R\begin{bmatrix}i_\alpha \\ i_\beta\end{bmatrix} + L\frac{d}{dt}\begin{bmatrix}i_\alpha \\ i_\beta\end{bmatrix} + \begin{bmatrix}u_{b\alpha} \\ u_{b\beta}\end{bmatrix} \quad \textbf{(2.7)}$$

Also,

$$C\frac{du_{dc}}{dt} = \frac{3}{2}\left[i_\alpha(t) + i_\beta(t)\right] - i_{load} \quad \textbf{(2.8)}$$

The above vector $\mathfrak{R}$ can be anything such as voltage or current.

Now, we shall convert the $\alpha\beta$ co-ordinate vector to dq, also known as Park's transformation, as follows:

$$\mathfrak{R}_{dq} = \mathfrak{R}_{\alpha\beta}.e^{-j\theta} \quad \textbf{(2.9)}$$

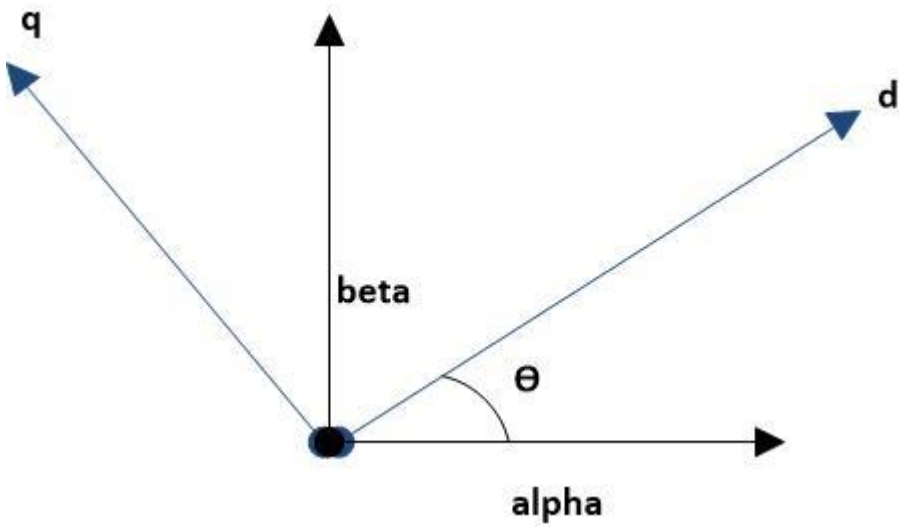

Fig. 6: dq and αβ frame of reference

Here,

$\Re_{dq}$ is the vector in dq frame of reference

And, $\Re_{\alpha\beta}$ is the vector in $\alpha\beta$-frame of reference.

On expanding, we get:

$$\Re_d + j\Re_q = [\Re_\alpha cos(\theta) + \Re_\beta sin(\theta)] + j[-\Re_\alpha sin(\theta) + \Re_\beta cos(\theta)] \quad \textbf{(2.10)}$$

As a result, we get the following equations for the above given system:

$$u_{sdq}.e^{j\theta} = R\, i_{dq}(t)e^{j\theta} + L\, e^{j\theta}\left[j\omega i_{dq} + \frac{di_{dq}}{dt}\right] + e^{j\theta}u_{bdq} \quad \textbf{(2.11)}$$

Equating the real and imaginary part, we get:

$$u_{sd} = Ri_d(t) + L\left[-\omega i_q + \frac{di_d}{dt}\right] + u_{bd} \quad \textbf{(2.12)}$$

$$u_{sq} = Ri_q(t) + L\left[\omega i_d + \frac{di_q}{dt}\right] + u_{bq} \quad \textbf{(2.13)}$$

Also,

$$C\frac{du_{dc}}{dt} = \frac{3}{2}\left[i_d(t) + i_q(t)\right] - i_{load} \quad \textbf{(2.14)}$$

2.2. MATHEMATICAL MODEL OF A RECTIFIER

The combination of the previous equations can be represented as a block diagram.

On applying Laplace transformation, we get:

$$\mathbf{U(s) = (R + sL).\, I(s)} \quad \textbf{(2.15)}$$

Also, we get:

$$\mathbf{C\ sV(s) = I(s) - I_{load}(s)} \quad \textbf{(2.16)}$$

The rectifier is being modeled as follows:

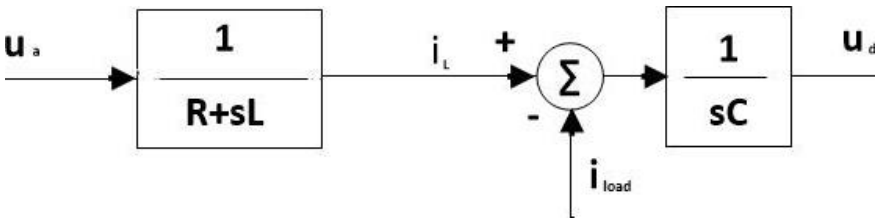

Fig. 7: Modeling of Rectifier

Here, $u = u_s - u_b$

2.3. MATHEMATICAL MODELLING OF CHOPPER

The buck converter is used in the project for dc to dc conversion. Modeling is done for both the modes: Mode 1 is when the switch is on and Mode 2 is when the switch is off.

After the averaging is done over a time period of T for a duty cycle of D, for both ON periods and OFF period.

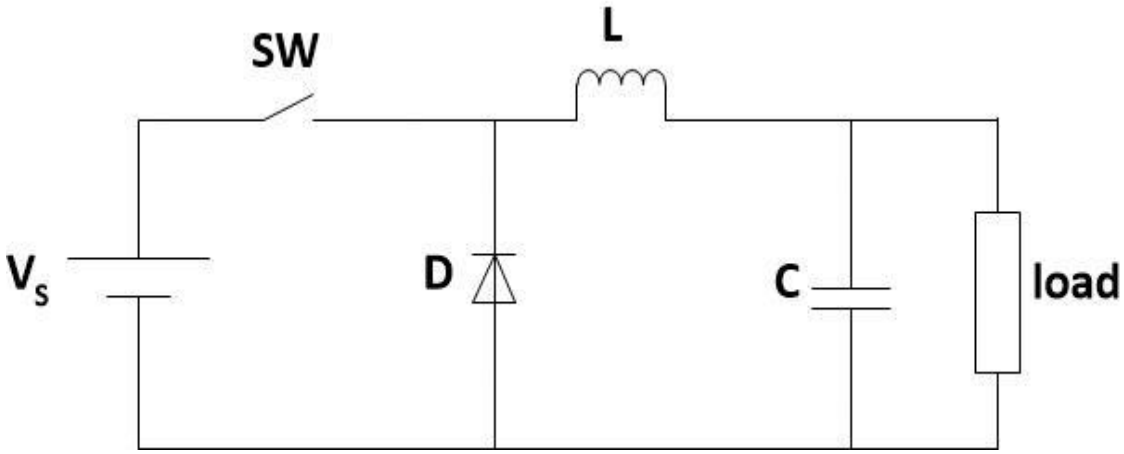

Fig. 8: Buck Converter

MODE I: SWITCH IS ON

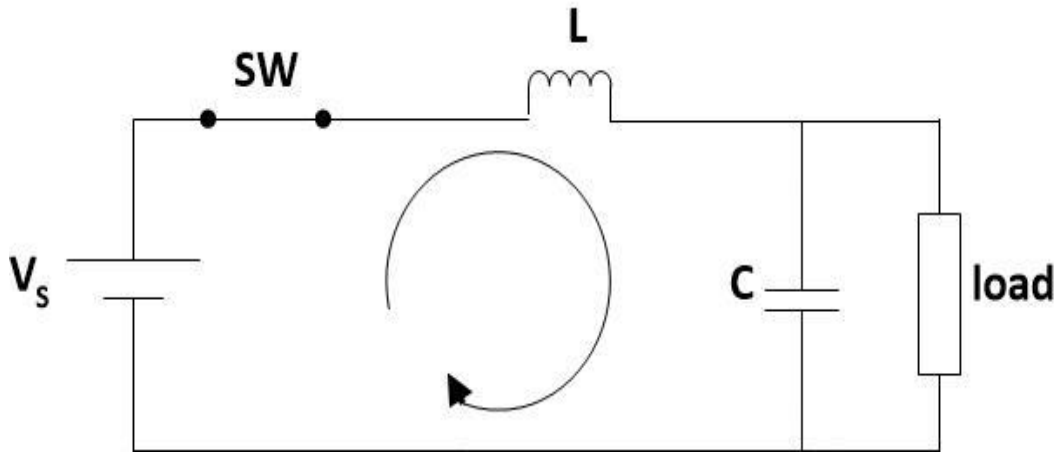

Fig. 9: Buck Converter operation with closed switch

When the switch is in the ON state, then by KVL in the loop shown below, we get the following equation:

$$V_S = L\frac{di_L}{dt} + V_O \qquad (2.17)$$

$$\mathbf{L}\frac{\mathbf{di_L}}{\mathbf{dt}} = \mathbf{V_S} - \mathbf{V_O} \quad \textbf{(2.18)}$$

Here, $V_C = V_S$

Also, by KCL at the node point of the capacitor, load and inductor L connection, we get:

$$\mathbf{i_L} = \mathbf{i_C} + \mathbf{i_o} \quad \textbf{(2.19)}$$

$$\Rightarrow \mathbf{C}\frac{\mathbf{dV_c}}{\mathbf{dt}} = \mathbf{i_L} - \mathbf{i_o} \quad \textbf{(2.20)}$$

Here, for the resistive load of R, we've:

$$\mathbf{i_o} = \frac{\mathbf{V_o}}{\mathbf{R}} \quad \textbf{(2.21)}$$

From the above two equations, we get the following state model for the mode 1:

$$\begin{bmatrix} \dot{i}_L \\ \dot{v}_C \end{bmatrix} = \begin{bmatrix} 0 & \frac{-1}{L} \\ \frac{1}{C} & \frac{-1}{RC} \end{bmatrix} \begin{bmatrix} i_L \\ v_C \end{bmatrix} + \begin{bmatrix} \frac{1}{L} \\ 0 \end{bmatrix} V_S \quad \textbf{(2.22)}$$

$$[V_O] = [0 \quad 1] \begin{bmatrix} i_L \\ V_C \end{bmatrix} \quad \textbf{(2.23)}$$

MODE II: SWITCH IS OFF

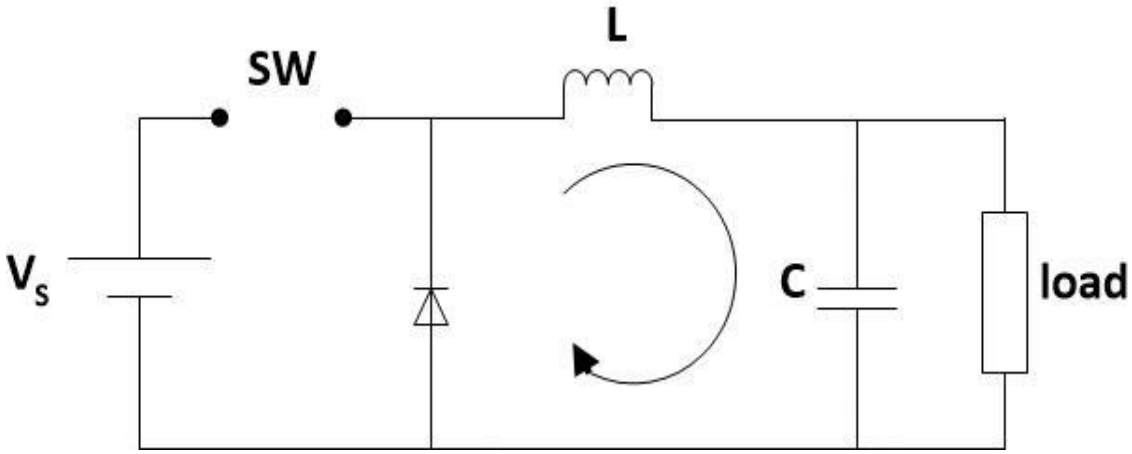

Fig. 10: Buck Converter operation with open switch

When the switch is OFF, then by KVL in the loop shown below, we have the following equation:

$$\mathbf{0} = \mathbf{L}\frac{\mathbf{di_L}}{\mathbf{dt}} + \mathbf{V_O} \quad \textbf{(2.24)}$$

$$\mathbf{L}\frac{\mathbf{di_L}}{\mathbf{dt}} = \mathbf{0} - \mathbf{V_O} \quad \textbf{(2.25)}$$

Also, by KCL at the point of junction of capacitor, inductor and the load, we obtain the following equation:

$$\mathbf{i_L = i_C + i_o} \quad \textbf{(2.26)}$$

$$\Rightarrow \mathbf{C\frac{dV_c}{dt} = i_L - i_o} \quad \textbf{(2.27)}$$

From the above two equations, we get the state model for the mode 2, as follows:

$$\begin{bmatrix} \dot{i}_L \\ \dot{v}_C \end{bmatrix} = \begin{bmatrix} 0 & \frac{-1}{L} \\ \frac{1}{C} & \frac{-1}{RC} \end{bmatrix} \begin{bmatrix} i_L \\ v_C \end{bmatrix} + \begin{bmatrix} 0 \\ 0 \end{bmatrix} V_S \quad \textbf{(2.28)}$$

$$[V_O] = [0 \quad 1] \begin{bmatrix} i_L \\ V_C \end{bmatrix} \quad \textbf{(2.29)}$$

Now, we average the state model of both the states. Mode 1, exists for time DT and mode 2 exists for a time (1-D)T.

On averaging, we obtain the following state model:

$$\begin{bmatrix} \dot{i}_L \\ \dot{v}_C \end{bmatrix} = \begin{bmatrix} 0 & \frac{-1}{L} \\ \frac{1}{C} & \frac{-1}{RC} \end{bmatrix} \begin{bmatrix} i_L \\ v_C \end{bmatrix} + \begin{bmatrix} \frac{D}{L} \\ 0 \end{bmatrix} V_S \quad \textbf{(2.30)}$$

$$[V_O] = [0 \quad 1] \begin{bmatrix} i_L \\ V_C \end{bmatrix} \quad \textbf{(2.31)}$$

2.4. DQ TO ALPHA-BETA CONVERSION

In dq to αβ conversion i.e. the conversion from dc to two phase rotating AC system is also required sometimes, in order to fulfill certain conditions. Hence, here we are performing that conversion. We know:

$$\mathbf{\Re_{dq} = \Re_{\alpha\beta} . e^{-j\theta}} \quad \textbf{(2.32)}$$

Hence we can deduce that:

$$\mathbf{\Re_{\alpha\beta} = \Re_{dq} . e^{j\theta}} \quad \textbf{(2.33)}$$

$$\mathbf{\Re_\alpha + j\Re_\beta = [\Re_d + j\Re_q].[\cos(\theta) + j\sin(\theta)]} \quad \textbf{(2.34)}$$

Equating the imaginary and real part, we get:

$$\mathbf{\Re_\alpha = [\Re_d \cos(\theta) - \Re_q \sin(\theta)]} \quad \textbf{(2.35)}$$

$$\mathbf{\Re_\beta = [\Re_d \sin(\theta) + \Re_q \cos(\theta)]} \quad \textbf{(2.36)}$$

2.5. SECOND ORDER GENERALIZED INTEGRATOR (SOGI)

In order to develop the control techniques in power electronic converters, constant regulation and monitoring of the new signals is required. In order to implement the control methods in the system, we need to have the knowledge of certain parameters such as angle, frequency, offset, etc. These parameters can be obtained using PLL but its practical implementation is tedious. Second order generalized integrators are the techniques used to generate the orthogonal signals which are the signals in quadrature with each other. It uses the technique of band-passing and orthogonalization of the periodic signals.

2.6. PHASE LOCKED LOOP (PLL)

The application of power converters in the generation, transmission and distribution system has increased tremendously over years. The power system, on one hand has a very high inertia and over-loading capacity, where as the power converters have very low inertia and a very low over-loading capacity. This creates a need for the continuous and quick tracking of the phase or frequency of the system, so that the utility along with the converters is not affected by the sudden or large variation of current or voltage of the system.

Synchronization of the grid is necessary with the system which includes the functioning of the converters. For the fulfillment of the synchronization purpose, the knowledge of the system frequency, amplitude and the phase angle is necessary. One of the conventional synchronization schemes depends upon the zero crossing detection schemes, which has not proved to be reliant enough over the years, due to regular and significant addition of the power converters to the grid which has changed the power quality as it used to be earlier.

Phase locked loop is applicable for both single phase and three phase as well. Since, we are dealing with the single phase only, thus for the purpose of this project, we'll be focusing on the single phase power-base phase locked loop. Single phase PLL consists of the phase detector which is built using which consists of a multiplier, operating on the input signal and the feedback signal. The multiplier helps in the generation of the two signals, mainly of high frequency and another is of low frequency. The high frequency is filtered out using a PID block which is tuned in order to obtain its inherent

low pass filtering property. This low frequency signal, then obtained, is sent to a voltage controlled oscillator which has an inbuilt integrator which generates the angular frequency. This angular frequency is sent to the inbuilt integrator which generates the phase at the output signal. Here, the PID block tries to reduce the error between the generated phase of the output signal and the phase of the input signal to the PLL and this helps in the maintaining the phase or frequency of the system and it’s quick tracking.

CHAPTER 3

THE CONTROLLING STRATEGIES

3.1: INTRODUCTION

With the introduction of new semiconductor devices and new controlling platforms, there is a continuous need of evolution in the controlling techniques in the both existing and to be invented. The first in the line is the diode rectifiers that operate without any control. After this, the thyristors came into the picture which are semi-controlled, analog control circuitry is used which can regulate the firing angle of these thyristors.

The power converters usage range into various sectors, from the space sectors to the industrial sectors to the residential sectors. In the transportation sectors, where this project is majorly heading towards, these converters are used in the electric vehicle, hybrid vehicles, trains, ship, aircraft, etc. As power switching frequencies increases, the digital controlling schemes with the scope of advanced control scheme starts replacing the analog controlling schemes.

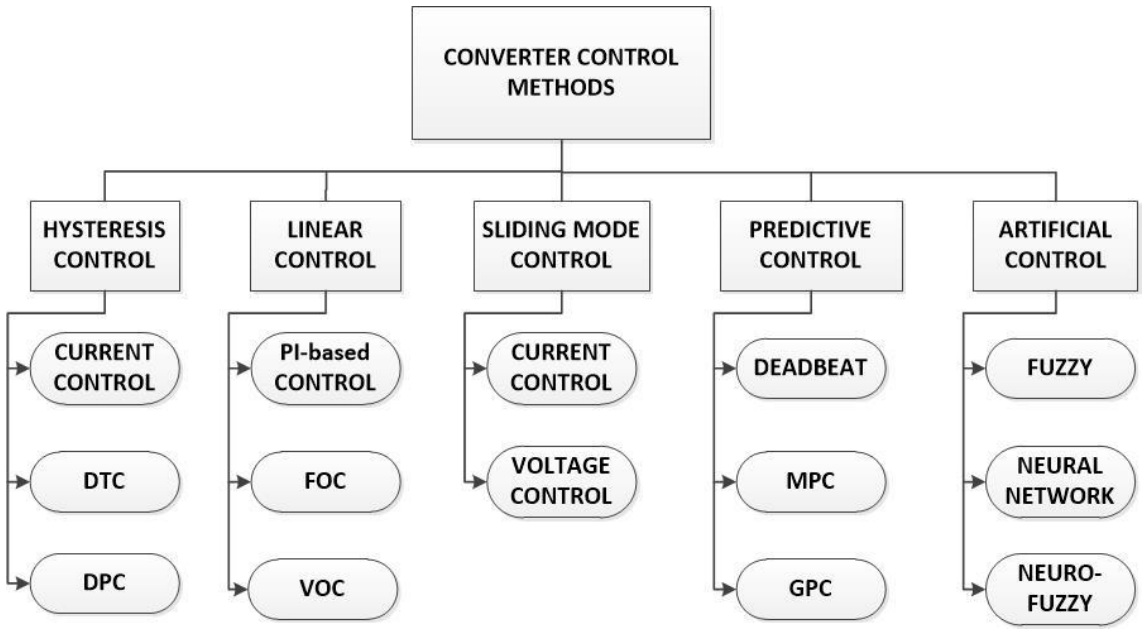

Fig. 11: Converter Control Methods

Now, we shall focus on the converter controllers' progress. The inception of the controlling in power converters starts with the controlling of the firing angle in

thyristors with the help of zero crossing detection. An extension of it came in the fully controlled switches such as IGBT (Insulated Gate Bi-polar Transistor) where the turn off is not supply dependant and controlled hard switching of the thyristor is possible and this controlled turn-off of the switches allows higher frequency and thereby lowers switching losses. One of the basic example of the controlling of the switch operation starts right from the switching control of a single switch, which can be seen in buck converter where the average lies in between zero and supply voltage value. This is maintained by controlling the duty cycle which is controlled by firing the switch at an instance when the triangular waveform is lower than the reference voltage. Here triangular waveform is of very high frequency.

The controlling method stated above is of the 1960s where the analog circuits are used consisting of the operational-amplifiers and passive components. Owing to the losses due to the passive components, with time, digital controlling came into existence. First they used to work in combination with the analog circuits [44]. But with the passage of time digital control is implemented completely. Microprocessors are most commonly used for the implementation of digital control in the power converters. Modern microcontrollers and the digital signal processors (DSP) have high computational capabilities and these are used for the implementation of intelligent control schemes.

The power converters have non-linear characteristics. However while taking the average of the output current or voltage, the converter is approximated to be a linear system and this is the basis of the most of the conventional control schemes existing today.

First of these control schemes is the Hysteresis control scheme. It ranges from the most basic current control to the direct torque control and direct power control. Hysteresis control here, takes the advantage of the non-linear characteristics of the power converters and it is used to determine the switching states of the semiconductor switches [7]. Implementation of the hysteresis control requires a very high frequency but this can lead to resonance problem resulting in the expenditure on the bulky filters [7].

Hysteresis control includes current control as the most basic type, direct power control and direct torque control as its sub-categories. Another category includes linear control. Linear control method employed in the power converters consider the approximation of

linearising the power converters. These include the conventional PI control method, the voltage oriented control method and the field oriented control method. These are the methods to which a beginner first gets to try their hands on. Before the implementation of any complex controlling methods, a system's controlled response is first checked using these methods. The control schemes which are linear in nature require additional coordinate transformation. Here, field oriented control (FOC) is the control method in which the frequency is variable. It is also known as the vector control method. Voltage oriented control (VOC) is applied to the converters which is connected to the grid. It is analogous to the field oriented control done in the case of induction motors. It guarantees fast transient response and better performance in the inner current control loop. Thus, the overall performance depends on the quality of the performance of inner current control loop. However, linear control system when applied to the non-linear system can introduce some unevenness in the dynamic performance of the converters.

Sliding Mode Control (SMC) can be used for both voltage control and current control. SMC is one of the control methods that works in compliance with the non-linear system which even the buck converter, which is ordinarily expected to be a linear system [9], behaving non-linearly works in sync with this controller. Sliding mode is advantageous over the traditional techniques in terms of robustness, easy implementation, better dynamic performance for large variations as well [9]. SMC possesses low sensitivity towards the plant and the variations in its parameters and also the disturbances which eliminates the need of system modeling. It also allows decoupling of the different parts of the system, leading to low complexity and providing a response which is independent of the parameters of the system [9]. However it has a slight disadvantage of the usage of additional hardware circuitry and deteriorated transient response due to the superposition of the ramp signal on the switching function of the sliding mode.

Neural network and fuzzy are the controlling techniques that form the pillar of artificial intelligent controllers in power electronic controllers. Fuzzy Logic Controller is based on fuzzy logic. Fuzzy logic was first implemented by Lotfi A. Zadeh. It is much similar to the human interpretation method. Since fuzzy logic is always subjective in nature, it remains vague and there's always a scope of improvement or non-attainment of the desired responses, depending upon the kind of fuzzy rules that are being formed and applied. As stated before, fuzzy logic is based on the degree of truth or falsity of the situation and is always relative in nature, where as Boolean logic has two discrete

values and concludes a statement to be either completely true or false. For the formation of fuzzy logic controller, it is first necessary to define or model a system such that it provides response similar to that of the actual system. Then the input and output regions are divided into many sections, called as fuzzy regions, which helps in determining the membership functions and defining the fuzzy sets and the universe of discourse in the fuzzy logic. This fuzzy set must have all the values ranging from 0 to 1 and thus a proper scaling of the input and output crisp values is desired. Depending upon the fuzzy sets and university of discourse available, the shape of the membership functions are also determined. Various membership function curves are available, such as triangular, Gaussian, trapezoidal, etc. Among these we have chosen the triangular membership function as it gives unique degree of membership for each of the fuzzy values and eliminates the ambiguity from the results.

3.2. THE PID CONTROLLING

The Proportional-Integrating-Derivative (PID) controller is a part of the linear controlling methods applied to the power converters. The present system consists of a rectifier, cascaded to a chopper via a dc link capacitor. Here the ac to dc rectifier is a nonlinear system and dc to dc converter is a linear system. The most basic and conventional type of controller used is the PID controller.

In electrical domain, linearity of a device is defined on the basis of the device voltage and current with respect to each other. A device is said to be linear only when the current flowing through the device forms a straight line when plotted against the voltage across the device. Here, the semiconductor switch is the device for which we don’t get a linear graph. Hence, the power converters are said to be a non-linear in nature.

PID control, on the other hand is the method applied to the devices which have a linear characteristic. The linear devices used can be a resistor or potentiometer, etc. Thus, in order to apply PID to the non-linear system, there has to be a way to make the system appear linear to the controller. The objective of the PID to be used here is to do a controlled switching of the switches involved. Thus, in order to do this Pulse Width Modulation (PWM) block is used. The job of PWM block is not only to control switching, but also linearizes the power converters [44]. Thus, here PWM works as a linear power actuator. Therefore, PI regulators are used with multi-loop systems which

is cascaded the drive system and the power converters [44].

In PID, every parameter has a different importance. The proportional parameter is responsible to decrease overshoot and decrease rise time as well. The role of integral parameter is to eliminate steady state error and decrease the rise time of the transient response. The differential parameter, on the other hand, is responsible for the decrease in the overshoot of the system response, and also it helps in decreasing the settling time of the transient response, thus giving the settled result in lesser time span.

Proportional (K_P)	**Integral (K_I)**	**Derivative (K_D)**
Decreases rise time	Eliminate steady state error	Decreases overshoot
Decreases overshoot	Decreases rise time	Decreases settling time

Table 3: Properties of the PID controller

The tracking of the reference is easier while using the PID controller, in case the signal and its reference are DC in nature. However, this controller gives a poor performance when the incoming signal has to track a sinusoidal reference which is present due to steady state error, present at frequencies other than that of DC. Also, it has incapability of reducing noise in the controlled signal. In PID, errors get accumulated from the past to which integral term gives a slow reaction. This prevents the system from reaching a set point within a smaller time frame.

3.2.1 Methodology

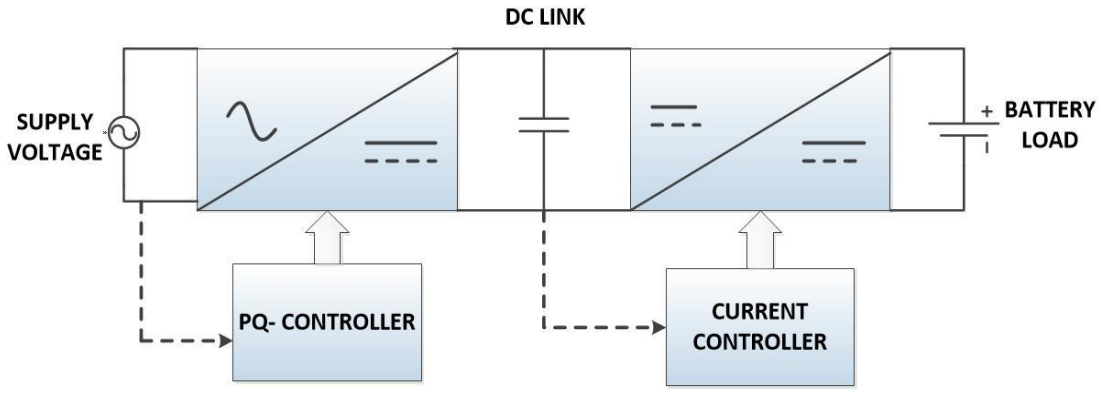

Fig. 12: Outline of the System Control via PID controller

The above figure depicts the system actually used in implementing the controlled charging scheme of the battery of an EV. There are two main parts of this system. First is the RECTIFIER, a device which helps in converting the AC signal into pulsating DC signal. The second part, which is connected to the rectifier in a cascaded manner, is the CHOPPER, a device which helps in the conversion of DC signal into a DC signal, both of which differ from the voltage level of the supply and the load.

In the PID controller, in general proportional-integral control is used and derivative parameter is not used. Because in PI control technique, derivative parameter function is included. It can be seen in the equation given below that the derivative parameter is inbuilt in the PI controller:

$$\mathbf{K_P + \frac{K_I}{s} = \frac{s\,K_P + K_I}{s}} \qquad \textbf{(3.1)}$$

The‘s’ parameter in the numerator is responsible for the derivative function in the PI controller itself. There are two sets of controlling techniques that is being implemented in this system. The first controlling is done of the rectifier and second controlling is done of the DC to DC converter. Active and reactive power control is done on the supply side in the rectifier and current controlling is done on the load side of the DC to DC converter.

PI is used in controlling the two cascaded system. The present system and controller allows controlling of the active and reactive power in all the four quadrants. The reference active and reactive power is considered as the command signals sent by the utility to the controller, defining the need of the active and reactive power required by the grid or being supplied by it.

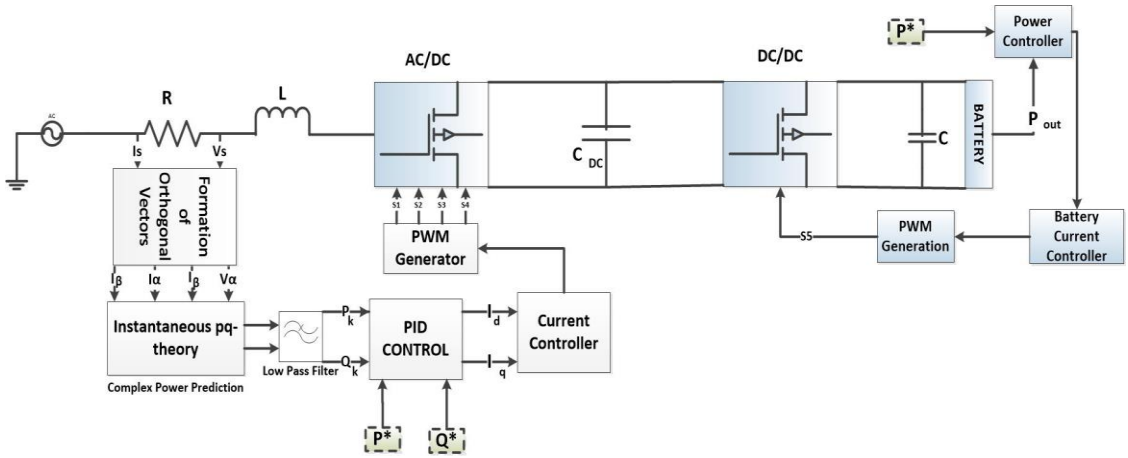

Fig. 13: Block diagram of complete PI controlled system

For the AC to DC rectifier, PI controller is employed to control the active and reactive power. In the above figure, we can see the schematic of the controller implemented in the whole system, where PI is implemented for each stage individually. In the first stage, we can see that there is a transformation from one system to another system. This is done in order to make the single phase AC signal DC, which is supported by the PI controllers as the follow of the sinusoid reference becomes difficult while using these controllers. In the first stage, after the transformation, an error is calculated and is sent to the controller to get zero steady state error and the output of these controllers is modified to get the current values in the transformed system. These current signals are transformed back into the system in which the plant operates and these signals are put into the current controllers, which are basically hysteresis controllers implemented to compare the grid current and the transformed current of the signals obtained from the PID block. This hysteresis controller generates the switching pulses for the MOSFETs used in the converter.

In the second stage of the conversion from a DC voltage level to another DC voltage level, PI controller is used again with the objective of controlling the battery or the load current at this stage. The general schematic of current control at the load end starts with the voltage control, the output of which is fed to the current controller. Here, however, the battery is connected at the load end. The battery, in general, is a very slow device and does not react immediately to the change in voltage across its terminals. It is for this reason, that the schematic of the current controller is changed. Instead of implementing voltage control, a power controller block is implemented. This power controller block

implemented is the PI controller, the output of which is adjusted to generate the reference current on the load side. The power reference given to generate the error is the same reference, which has been used in the controlling of power in the AC to DC conversion stage. The error generated between the reference power and the power of the load side of the DC to DC converter [56] is fed to the PI block, which generates a signal equivalent to the battery current. This battery current fed by the controller is considered as the reference and is compared with the actual load side current of the converter and this error is fed to another PI block, which again tries to get a zero steady state error. This PI block generates switching pulses for the MOSFET used in DC voltage level converter.

3.3 THE MODEL PREDICTIVE CONTROLLING

The approach of MPC (Model Predictive Controlling) is quite different from the conventional PI control in terms of energy processing and the way they assume the power converter to behave. The MPC controller considers the power converter to be non-linear device and a discontinuous actuator. The controlling action using MPC is taken considering only single controller which is implemented in a discretized model as the minimized cost function. MPC allows optimization of one or more parameters that are required to be controlled in the system. As stated before, that PI controller requires a different set of PWM blocks in order to allow linear performance of the converter with respect to the controller. MPC controller has an advantage over the conventional one in a way that it does not require a separate PWM block. The cascaded multi-PI loop that was often required in the controlling of the plant parameters can be easily taken over by the single loop controller. MPC offers software based optimal solution, simplicity and flexibility which can be costly but it is adjustable based on its coping capacity with the recent and fast developments of the processor capacities.

The implementation of MPC complies with many applications having different control requirements. Current control, power control, control of low switching frequencies, torque control, voltage control, flux linkage control, etc are few of the control requirements of the power converters. For this purpose, cost function is defined which is usually a measure of error between the reference and the predicted variable, such as current error, power error, frequency error, voltage error, torque error, etc. Thus

predictive control is advantageous on different kinds of variables and allows implementation of restrictions on all these types.

MPC predicts the behaviour of the controlled variables in future within a stipulated horizon in time. Here, a cost function is defined which contains the definition of the controlled variable. In MPC (Model Predictive Control), concepts are very simple and intuitive. It defines the desired behaviour of the system. The cost function defined is minimised to obtain an optimal solution. By using predictive control it is possible to avoid the cascaded structure which is typically used in a linear control scheme. This helps in obtaining very fast transient responses. An example of this is speed control using trajectory-based predictive control. The non-linearities in the system can be included in the model which avoids the need to linearise the model for a given operating point, and improves the operation of the system for all the variables.

Few of the noted advantages of the controller include:

1. Easy synchronism with the non-linearity of the plant model
2. Intuitive and easy to understand concepts
3. Easy implementation
4. Easy modification and extension
5. More than one variable can be focussed at, at a time
6. Constraints can be easily treated
7. Dead times can be compensated

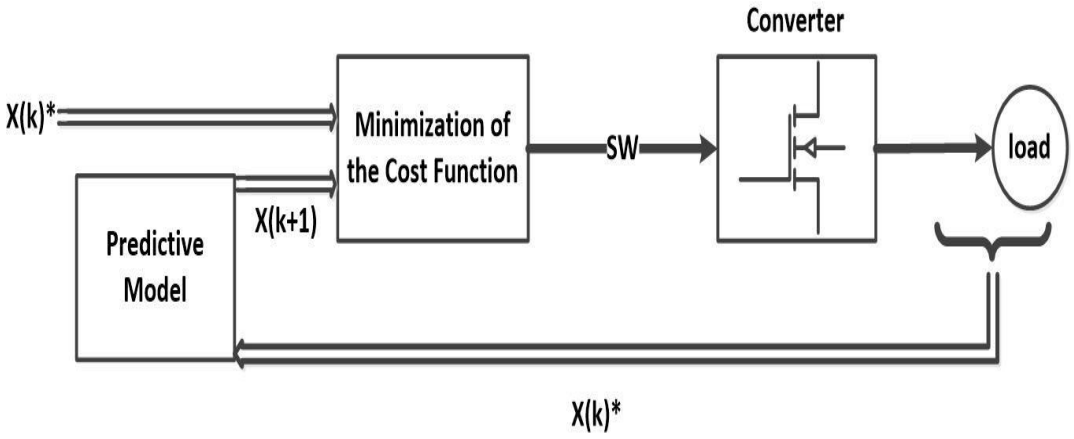

Fig. 14: General MPC scheme

Following steps are identified in the designing of the MPC control set:

1. Finding out the plant model
2. Identify the possible switching states and the relation of switching to the input or output voltage and current
3. Desired behaviour of the system is defined in cost function
4. Discretization of the model obtained in order to predict the future behaviour of the plant
5. Selection of the switching states that minimizes the cost function

3.3.1. Methodology

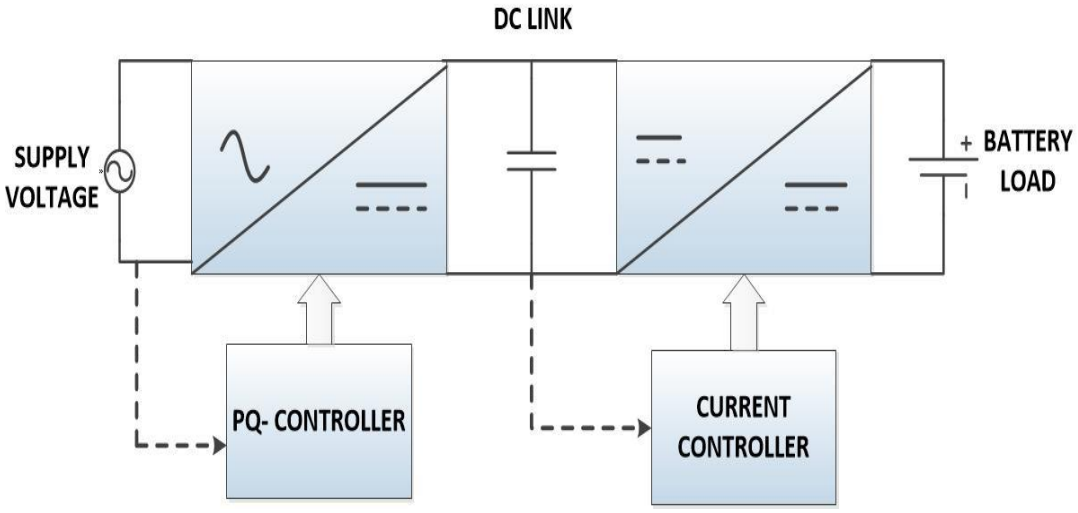

Fig. 15: Block diagram of MPC controlled system

The above figure shows the plant along with the controlling implemented in both the stages. Active and reactive power control is done in the first stage and current control is done in the second stage. In this segment, in the above figure, the model predictive controller is applied at both the stages.

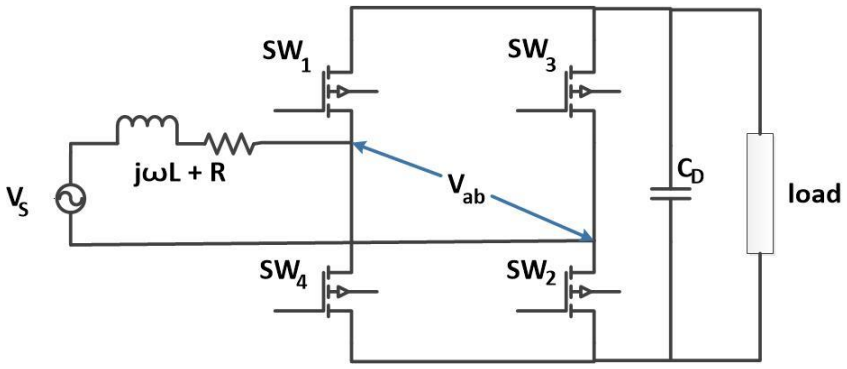

Fig. 16: The Single Phase Rectifier

The fig. 3 shows the topology of the first stage single phase off board charging controller. The first stage is the single phase Fig. 3. Topology of the PWM converter ac to dc converter, comprising of the MOSFET switches with the anti-parallel diodes. This is followed by step down DC voltage regulator comprising the second stage, which regulates the voltage up to the nominal voltage of the battery. The single phase balanced supply is connected to the converter via an inductor (L_S), in series with a small resistance value. This output of ac to dc converter is fed to the dc to dc converter via a dc link capacitor [19]. The output from the second stage is fed to the battery via an inductor and a capacitor in parallel. The first stage is to transform from single phase to α-β transformation using Clark's transformation theory. However, since here we have only single phase thus we take α vector as the single phase voltage itself and for the β vector, we obtain it by transforming the source voltage vector by 90 degrees By KVL in the above circuit at the source end we get,

$$\mathbf{L_S \frac{di_S}{dt} = v_S - V_{AB} - i_S(t)R_S} \quad \textbf{(3.2)}$$

Here, the source voltage is given by

$$\mathbf{v_s(t) = V_S cos(\omega t)} \quad \textbf{(3.3)}$$

For the single phase we obtain apparent power of the system as follows:

$$\mathbf{S = P + jQ = v_s i_s^*} \quad \textbf{(3.4)}$$

And we've,

$$\mathbf{i_s = I_s cos(\omega t - \varphi) + \sum_{k=2n+1}^{\infty} I_{sk} cos(k\omega t - \varphi_k)} \quad \textbf{(3.5)}$$

As a result, we obtain active and reactive power as following

$$\mathbf{P = \frac{V_{sm} I_{sm} cos\varphi}{2}} \quad \textbf{(3.6)}$$

$$\mathbf{Q = \frac{V_{sm} I_{sm} sin\varphi}{2}} \quad \textbf{(3.7)}$$

where,

$\mathbf{V_S}$ is the source voltage,

$\mathbf{I_S}$ is the source current,

$\boldsymbol{\varphi(t)}$ is the phase angle,

$\mathbf{V_{sm}}$ is the peak value of source voltage,
$\mathbf{I_{sm}}(t)$ is the peak value of source current,

P and **Q** is the active and reactive power flowing from the source towards the battery, and, $\mathbf{i_s}$ denotes the complex conjugate of the source current [53].

In three phase system, the α-β components can be obtained using instantaneous-pq theory. Taking a cue from it, we can obtain the two above said components for single phase system as well, by constructing a virtual two-phase system. Thus, rewriting active and reactive power in the terms of α-β component, we obtain:

$$\mathbf{P} = \frac{\mathbf{v_{s\alpha} i_{s\alpha} + v_{s\beta} i_{s\beta}}}{\mathbf{2}} \tag{3.8}$$

$$\mathbf{Q} = \frac{\mathbf{v_{s\beta} i_{s\alpha} - v_{S\alpha} i_{s\beta}}}{\mathbf{2}} \tag{3.9}$$

Here, the obtained α-component of the source voltage and current are the sensed signals and the β-component is the one quarter of the time delay of the α-components of source voltage and current. Another way of obtaining the components is by using Hilbert transformation, second order generalized integrator (SOGI), all pass filter. Here, SOGI is an advanced technique of orthogonal signal generation. We can obtain the α-β component using SOGI by implementing the following transfer functions:

$$\mathbf{t}_{\alpha}(\mathbf{s}) = \frac{\mathbf{k\omega}}{\mathbf{s^2 + 2\omega s + \omega^2}} \tag{3.10}$$

$$\mathbf{t}_{\beta}(\mathbf{s}) = \frac{\mathbf{k\omega}}{\mathbf{s^2 + 2\omega s + \omega^2}}\mathbf{s} \tag{3.11}$$

Here, using the above equations, we obtain $v_{s\alpha}$, $v_{s\beta}$, $i_{s\alpha}$ and $i_{s\beta}$. Now, taking the derivative of both the sides of equations (3.8) and (3.9) with respect to time (t) respectively, we get:

$$\frac{\mathbf{dP}}{\mathbf{dt}} = \frac{\mathbf{1}}{\mathbf{2}}\left[\mathbf{v_{s\alpha}}\frac{\mathbf{di_{s\alpha}}}{\mathbf{dt}} + \mathbf{i_{s\alpha}}\frac{\mathbf{dv_{s\alpha}}}{\mathbf{dt}} + \mathbf{v_{s\beta}}\frac{\mathbf{di_{s\beta}}}{\mathbf{dt}} + \mathbf{i_{s\beta}}\frac{\mathbf{dv_{s\beta}}}{\mathbf{dt}}\right] \tag{3.12}$$

$$\frac{\mathbf{dQ}}{\mathbf{dt}} = \frac{\mathbf{1}}{\mathbf{2}}\left[\mathbf{v_{s\beta}}\frac{\mathbf{di_{s\alpha}}}{\mathbf{dt}} + \mathbf{i_{s\alpha}}\frac{\mathbf{dv_{s\beta}}}{\mathbf{dt}} - \mathbf{v_{s\alpha}}\frac{\mathbf{di_{s\beta}}}{\mathbf{dt}} - \mathbf{i_{s\beta}}\frac{\mathbf{dv_{s\alpha}}}{\mathbf{dt}}\right] \tag{3.13}$$

With the help of above two equations, we obtain $S_{(k+1)}$ which is $P_{(k+1)}$ and $Q_{(k+1)}$. Thus, we can obtain error in terms of square of magnitudes of apparent power using the values

at k_{th} instant and this is used to calculate the values at $(k+1)_{th}$ instant. We obtain a cost function of the active and reactive powers as follows:

$$\mathbf{C.F} = |\mathbf{S_{ref}^{k}} - \mathbf{S^{k+1}}|^2 \quad \textbf{(3.14)}$$

Thus we get,

$$\mathbf{C.F} = |\mathbf{P_{ref}^{k}} - \mathbf{P^{k+1}}|^2 + |\mathbf{Q_{ref}^{k}} - \mathbf{Q^{k+1}}|^2 \quad \textbf{(3.15)}$$

Here C.F is the cost function.

This includes the error of between the estimated next state values to that of the present state value. The square of the error allows increasing the accuracy and precision in predicting the values to be used for the estimation of the next state.

$\boldsymbol{\gamma}$ is the weighing factor, which is included in cost function and is used to tune the importance or the cost of the function, here reactive power q to be specific, in relation to that of the control of active power. The value of $\boldsymbol{\gamma}$ is to be tuned properly in order to get a desired performance. There is no such standard formula on which the setting of the weighing factor can be done. However there are some basic guidelines to establish the value of the weighing factor, which can improve the effectiveness of the MPC on the system. But, this empirical method does not necessarily gives the best possible result. Hence, there is an approach to reduce the effect of weighing factor in the control of active and reactive power is being used in the following manner.

3.3.2. Optimization of Cost Function

In the above equation, where the cost function is defined, the aim is to optimise the flow of active and reactive power and for that purpose, we take the first step is to build an equation that can predict future values. We can write future values using discrete time model in terms of following equation:

$$\mathbf{S^{k+1}} = \mathbf{S^{k}} + \mathbf{T_s}\frac{\mathbf{dS^{k}}}{\mathbf{dt}} \quad \textbf{(3.16)}$$

Here, T_s is the sampling time. Re-writing the above equation in terms of active and reactive power for the $(k+1)_{th}$ terms, we've:

$$\mathbf{P^{k+1}} = \mathbf{P^{k}} + \mathbf{T_s}\frac{\mathbf{dP^{k}}}{\mathbf{dt}} \quad \textbf{(3.17)}$$

$$\mathbf{Q^{k+1} = Q^{k} + T_s \frac{dQ^k}{dt}} \quad \textbf{(3.18)}$$

Now, extracting α and β components of source current ($\mathbf{i_s}$) and re-writing equation (3.2) for the α-β components, we get:

$$\mathbf{\frac{di_{s\alpha}}{dt} = \frac{1}{L_s}[v_{s\alpha} - v_{ab\alpha} - i_s R_s]} \quad \textbf{(3.19)}$$

$$\mathbf{\frac{di_{s\alpha}}{dt} = \frac{1}{L_s}[v_{s\alpha} - v_{ab\alpha} - i_s R_s]} \quad \textbf{(3.20)}$$

Substituting these values from equations (3.19) and (3.20) in equations (3.12) and (3.13), we've:

$$\mathbf{\frac{dP}{dt} = \frac{1}{2L_s}\left[V_{sm}^2 - \left(v_{s\alpha}v_{ab\alpha} + v_{s\beta}v_{ab\beta}\right) - 2R_sP\right] - Q\omega} \quad \textbf{(3.21)}$$

$$\mathbf{\frac{dQ}{dt} = -\frac{1}{2L_s}\left[\left(v_{s\beta}v_{ab\alpha} - v_{s\alpha}v_{ab\beta}\right) - 2R_sQ\right] + P\omega} \quad \textbf{(3.22)}$$

Substituting values of equations from (3.21) and (3.22) into equations (3.17) and (3.18), we obtain:

$$\mathbf{P^{k+1} = P^{k} - T_sQ_k\omega + \frac{T_s}{2L_s}\left[V_{sm}^2 - v_{s\alpha}v_{ab\alpha} - v_{s\beta}v_{ab\beta}\right]} \quad \textbf{(3.23)}$$

$$\mathbf{Q^{k+1} = Q^{k} + T_sP_k\omega - \frac{T_s}{2L_s}\left[v_{s\beta}v_{ab\alpha} - v_{s\alpha}v_{ab\beta}\right]} \quad \textbf{(3.24)}$$

In the above stated equations, P^k and Q^k are active and reactive powers at the k^{th} time interval with a sampling time of T_s. And P_{k+1} and Q_{k+1} is the active and reactive powers to be calculated or estimated at the $(k + 1)_{th}$ time interval. These values when substituted in equation (3.15), provides us with cost function. The cost function that will be obtained in the equation (3.15) upon substitution of the derivatives of P and Q, will give the error between present instantaneous value and the next predicted state. The error given by the equation will be penalised even for a small value of error. That is to say, even for a small change in the value of control variable from that of the reference values, the system responds quickly, which means that frequency increases. Needless to say, it will give a faster controller response. Now, for the optimization purpose, the derivative of the cost function is required to be found by selecting the appropriate control variable. However, the differentiation of the cost function given in equation

(3.15) will be complex. Hence, in order to achieve simplicity, cost function is modified as follow:

$$\boldsymbol{C.F.} = |\boldsymbol{P_{ref}^{k}} - \boldsymbol{P^{k+1}}| + \boldsymbol{\gamma}\,|\boldsymbol{Q_{ref}^{k}} - \boldsymbol{Q^{k+1}}| \qquad \textbf{(3.25)}$$

The above equation is the cost function defined which is used in this project. There is another way of declaring the cost function that allows greater compensation for the deviation of error from a zero steady state. It is expressed in the following equation:

$$\boldsymbol{C.F.} = |\boldsymbol{P_{ref}^{k}} - \boldsymbol{P^{k+1}}|^{2} + \boldsymbol{\gamma}\,|\boldsymbol{Q_{ref}^{k}} - \boldsymbol{Q^{k+1}}|^{2} \qquad \textbf{(3.26)}$$

The problem with the above equation is that in the process of minimization of the cost function, the calculation for the condition of the minimization becomes complex. For this reason we don't use the above cost function.

For simplicity, we take the value of weighing factor as unity. Now, selecting $v_{ab\alpha}$ and $v_{ab\beta}$ as the control variables, we calculate the modulation function in the following manner:

$$\frac{\partial\, \mathbf{C.F.(k)}}{\partial \mathbf{v_{ab\alpha}(k)}} = \mathbf{0} \qquad \textbf{(3.27)}$$

$$\frac{\partial\, \mathbf{C.F.(k)}}{\partial \mathbf{v_{ab\beta}(k)}} = \mathbf{0} \qquad \textbf{(3.28)}$$

We get the following equations modulation function,

$$\mathbf{m_F(k)} = \frac{\mathbf{u_{s\alpha}(k)U_{sm}^{2}T_s + 2\omega LT_s[P(k)u_{s\beta}(k) - Q(k)u_{s\alpha}(k)] - 2L[P_{ref}(k) - P(k)]u_{s\alpha}(k) - 2L[Q_{ref}(k) - Q(k)]u_{s\beta}(k)}}{\mathbf{u_{dc}(k)U_{sm}^{2}T_s}} \qquad \textbf{(3.30)}$$

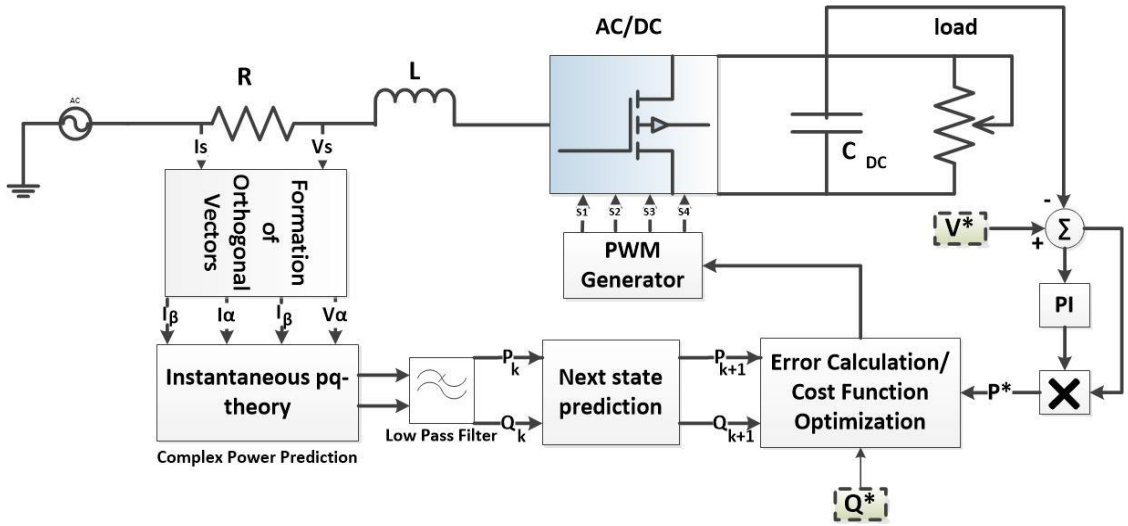

Fig. 17: Block diagram of the MPC controlled rectifier

The above block diagram shows the implementation of the MPC to the rectifier system. The R-load in the diagram represents the load connected to the system. In our case, the load is the DC to DC converter with battery connected on the load side of the chopper.

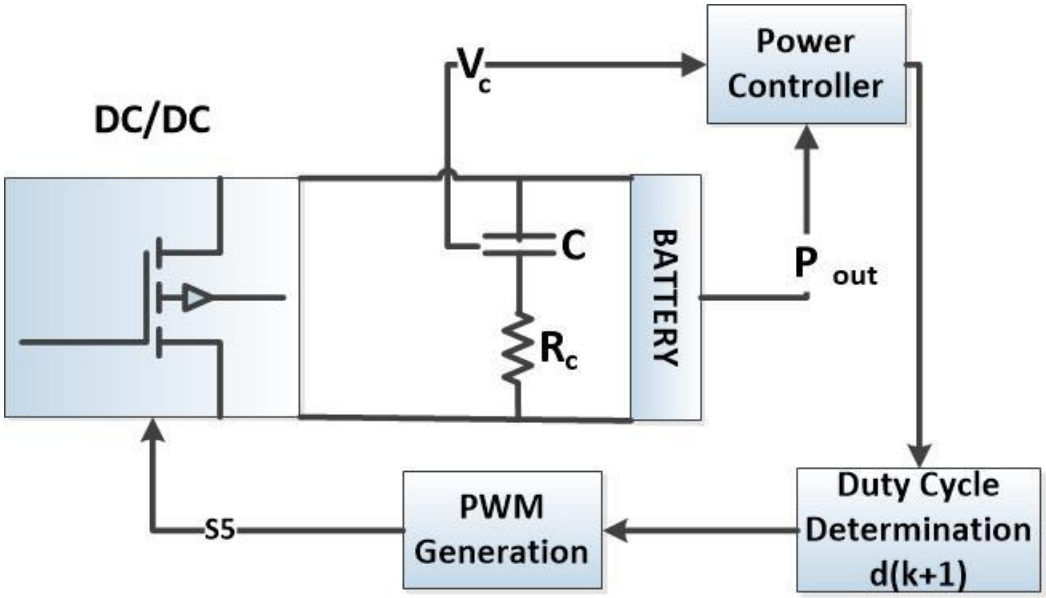

Fig. 18: Block diagram of MPC controlled DC to DC converter

The above diagram shows the model predictive controlling of the chopper. The steps followed in the development of the controlling block for the DC to DC converter is given below:

1. It starts with the modeling of the converter in the discrete domain.

2. Define the cost function of the model predictive control with the help of simplified model in discrete time domain.
3. Select the control variable and minimize the cost function.
4. Solve the obtained equations to get the desired results.
5. Modify the equation according to the practical requirements.

Taking the first step in the construction of the controlling block of the converter, we've already obtained a discrete state space model of the converter. It is as follows:

$$\begin{bmatrix} \mathbf{i_L} \\ \mathbf{\dot{v}_C} \end{bmatrix} = \begin{bmatrix} \mathbf{0} & \mathbf{\frac{-1}{L}} \\ \mathbf{\frac{1}{C}} & \mathbf{\frac{-1}{RC}} \end{bmatrix} \begin{bmatrix} \mathbf{i_L} \\ \mathbf{v_C} \end{bmatrix} + \begin{bmatrix} \mathbf{\frac{D}{L}} \\ \mathbf{0} \end{bmatrix} \mathbf{V_S} \tag{3.31}$$

$$[\mathbf{V_O}] = \begin{bmatrix} \mathbf{0} & \mathbf{1} \end{bmatrix} \begin{bmatrix} \mathbf{i_L} \\ \mathbf{V_C} \end{bmatrix} \tag{3.32}$$

The above model is obtained by averaging technique, considering the working of the converter in both the states i.e. when switch is ON and when switch is OFF. However, for the controller designing we need to develop a discrete model, which also allows the forecasting of the operation states of a system and analyzing characteristics of the operations. In this, state space equations are written for both the continuous and discontinuous modes using the averaging technique. A resulting equation is obtained in terms of the exponential function. These equations are then linearized by ignoring the higher order terms of the exponent. We get the following equations:

$$\mathbf{x(k+1) = A\,x(k) + \ BV_{in}} \tag{3.33}$$

Where,

$$\mathbf{A} = \begin{bmatrix} \mathbf{1} & \mathbf{-\frac{T}{L}} \\ \mathbf{\frac{T}{C}} & \mathbf{1 - \frac{T}{RC}} \end{bmatrix}, \mathbf{B} = \begin{bmatrix} \mathbf{\frac{T\,d(k)}{L}} \\ \mathbf{0} \end{bmatrix} \tag{3.34}$$

$$\mathbf{x(k)} = \begin{bmatrix} \mathbf{\dot{I}_L} \\ \mathbf{\dot{v}_c} \end{bmatrix} \tag{3.35}$$

On expanding the above iterative equations we get:

$$\mathbf{i_L(k+1) = \ -\frac{T}{L} v_c(k) + \ i_L(k) + \frac{T\,d(k+1)}{L} V_{in}} \tag{3.36}$$

$$\mathbf{v_c(k+1) = \left(1 - \frac{T}{RC}\right) v_c(k) + \frac{T}{C} i_L(k)} \quad \textbf{(3.37)}$$

Now, for the current control purpose, we define cost function as follows:

$$\mathbf{C.F._2 = (i_L(k+1) - I_{ref})^2} \quad \textbf{(3.38)}$$

Where, $\mathbf{I_{ref} = V_{ref} / R}$

Here, we select d(k) i.e. duty cycle as the control variable. On minimizing the cost function, we've:

$$\mathbf{d_P(k+1) = \frac{T v_c(k) + L\,(I_{ref} - i_L(k))}{T\,V_{in}}} \quad \textbf{(3.39)}$$

In the above equations, the parameters defined were as follows:

C is the capacitance across the load, L is the inductance, f is the switching frequency, V_{in} is the input voltage, T is the time of the switching cycle. These parameters are used in the ideal scenario. In practical environment, there exist few of the parasitic parameters, such as the inductor resistance, capacitor resistance inbuilt in the inductors and the capacitors. Based on the inherent capacitive and inductive resistance, we obtain the following modified cost function:

$$\mathbf{C.F._2 = (i_L(k+1) - I^*_{ref})^2} \quad \textbf{(3.40)}$$

Here, $\mathbf{I_{ref}}$ is changed.

$$\mathbf{I^*_{ref} = \frac{V^*_{ref}}{R} = \frac{V_{ref} + err(k)}{R}}$$

$$\mathbf{= \frac{V_{ref} + v_c(k) - u_o(k)}{R}} \quad \textbf{(3.41)}$$

As a result we obtain following modified inductor current:

$$\mathbf{i^*_L(k+1) = \frac{T v_c(k) + L\,(I^*_{ref} - i_L(k))}{T\,V_{in}}} \quad \textbf{(3.42)}$$

Now, by minimizing the modified cost function, we obtain an equation for modified duty cycle:

$$\mathbf{d_P^*(k+1)} = \frac{\mathbf{Tv_c(k)+L\,(I_{ref}^* - i_L(k))}}{\mathbf{T\,V_{in}}} \qquad \textbf{(3.43)}$$

The deviation in error, between the actual output and the predicted output, obtained is due to the parametric deviation which is mainly because of the presence of parasitic parameters. Based on the simplified model, the expected value is modified in accordance with the change in err(k). In order to eliminate this deviation and to make err(k) to be zero, the control variable d(k+1) is provided that adjusts accordingly in the modified reference of the model.

CHAPTER 4

SIMULATION AND IMPLEMENTATION

4.1 PARAMETERS

Parameters	Values
Source Voltage (peak)	120 V
Source Inductance (L)	4 mH
DC Link Capacitor	400 µF
Capacitor near battery (Co)	47 µF
Rectifier switching frequency	24 kHz
DC-DC converter switching frequency	20 kHz

Table 4: Converter Parameters

Parameters	Values
Battery Nominal Voltage	100 V
Battery SoC	50 %
Battery Ampere-hour	30 A-h
DC Link Voltage	200 V

Battery side filter inductor	100 μH

Table 5: Battery Parameters

4.2 PI CONTROLLED SYSTEM

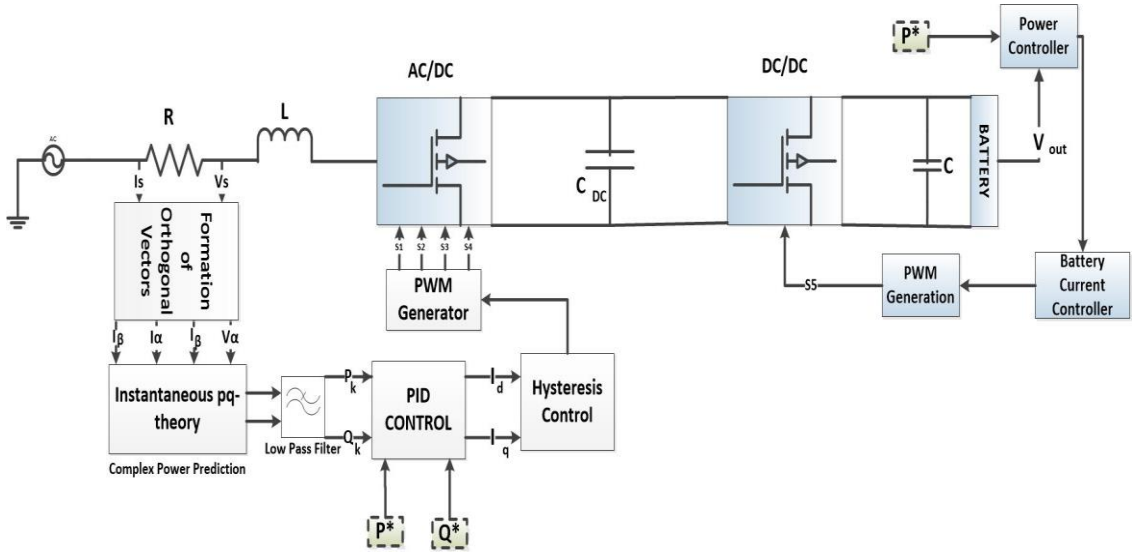

Fig. 19: Block diagram of the PID controlled charging system

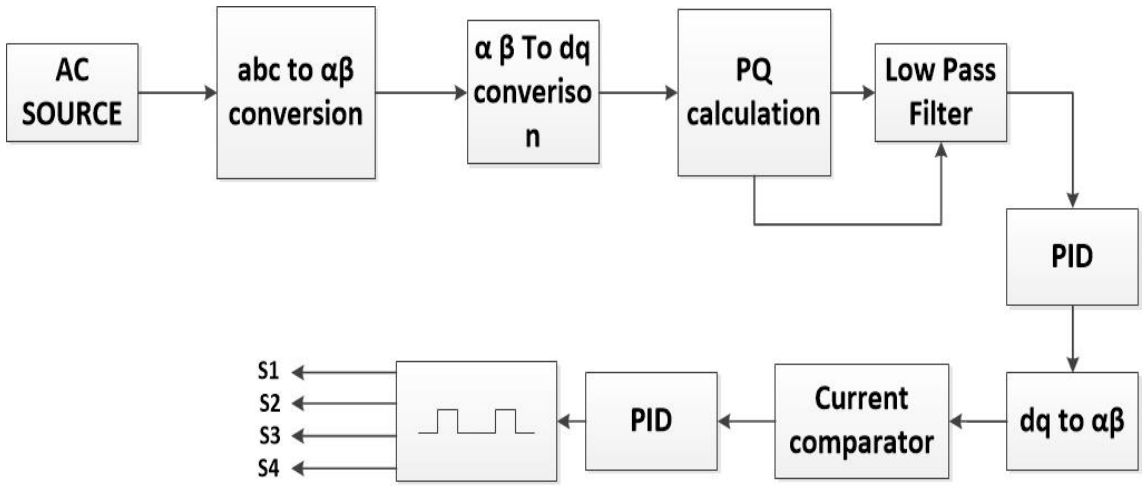

Fig. 19: Rectifier Controller

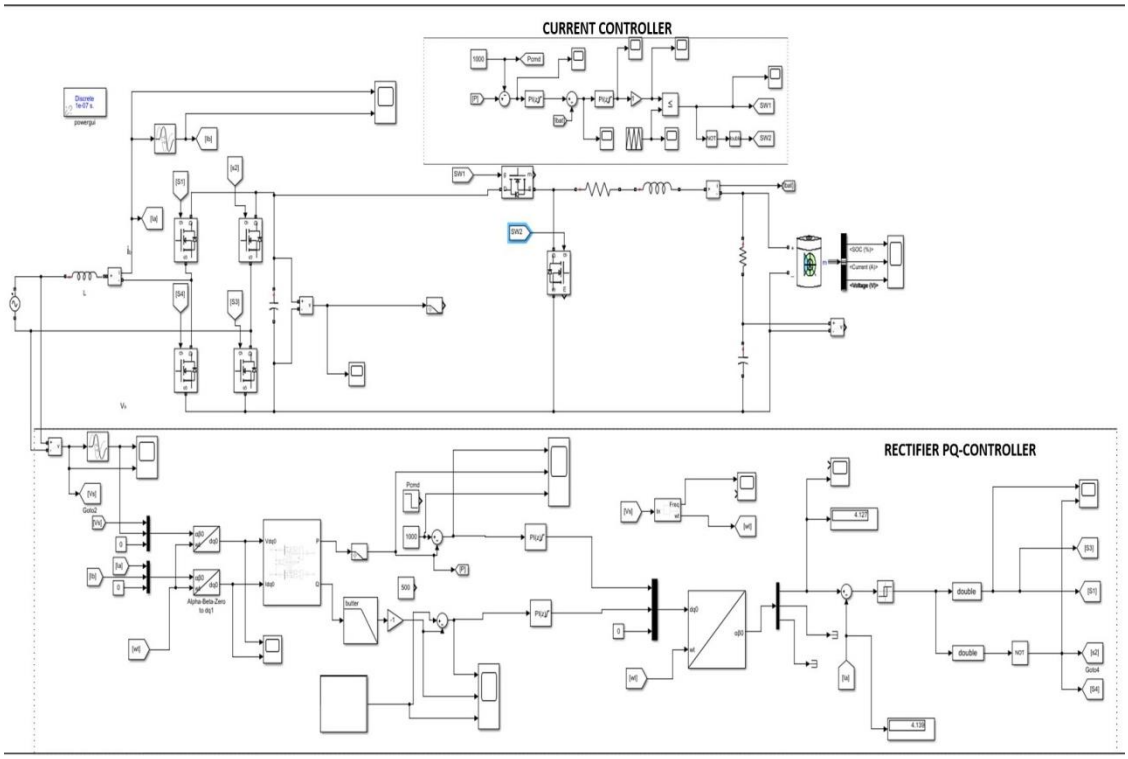

Fig. 20: Simulink Model of the PID controlled charger system

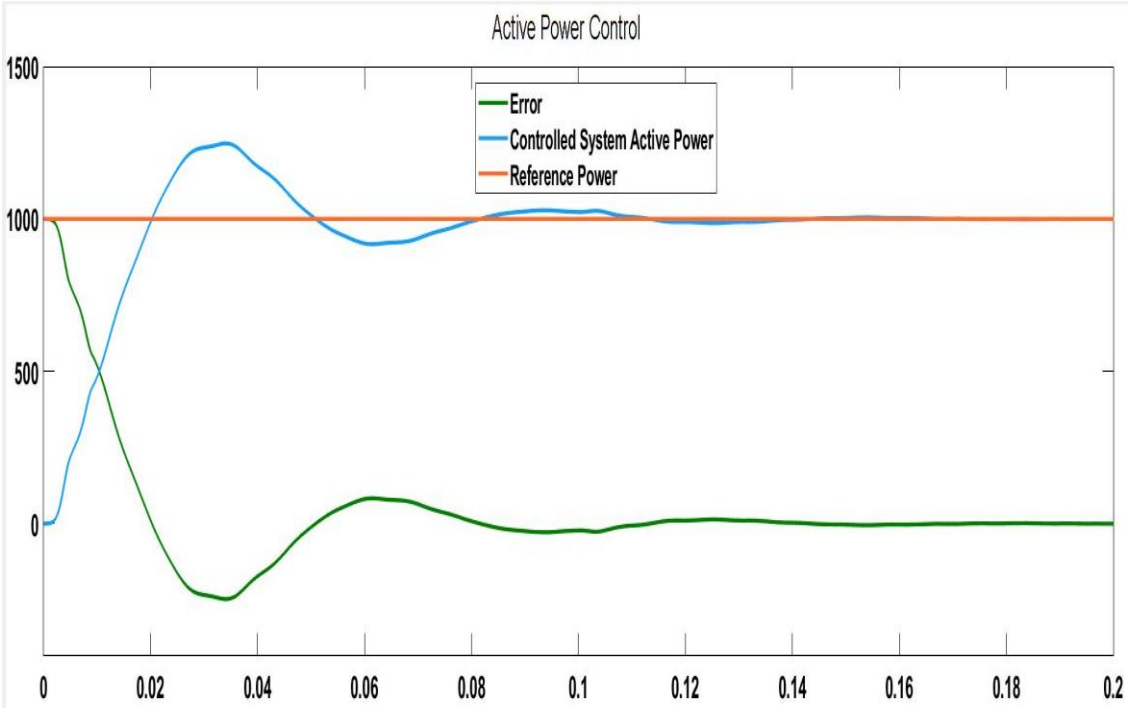

Fig. 21: Active Power Control Comparison

The above figure shows that it has an overshoot of 20% and settling time is around 0.175 seconds.

In the output of reactive power control, we can see that system settles around 0.55 second and we have attained zero steady state error.

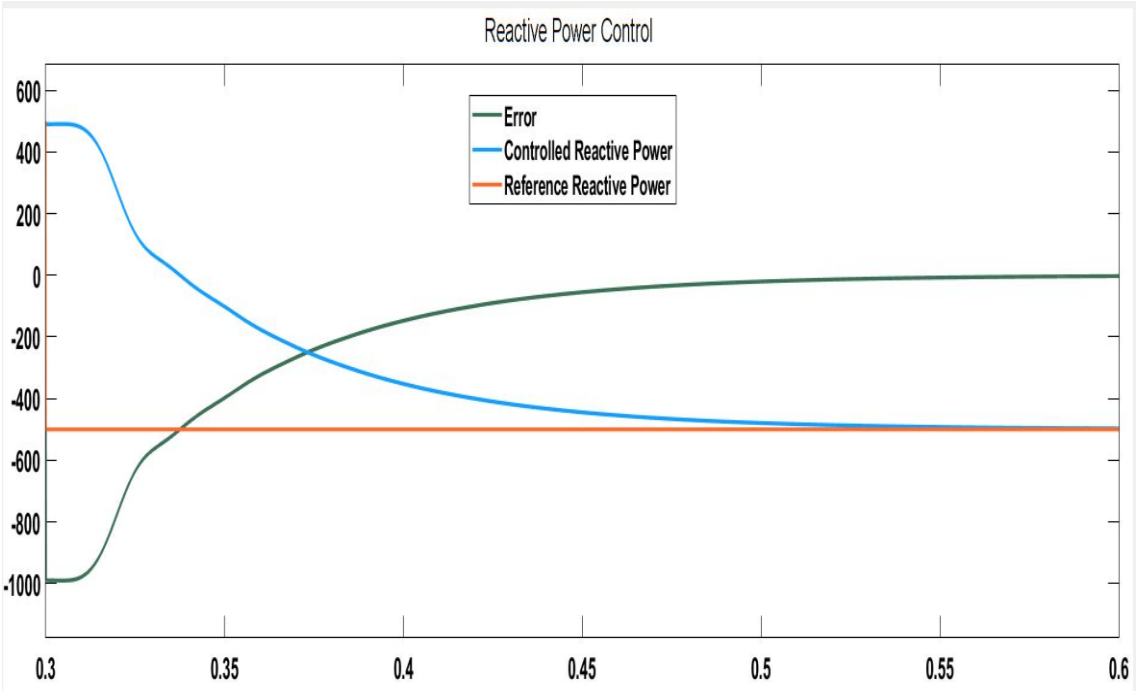

Fig. 22: Reactive Power Control Comparison

The figure given below shows that error goes to zero for the current control of the buck converter.

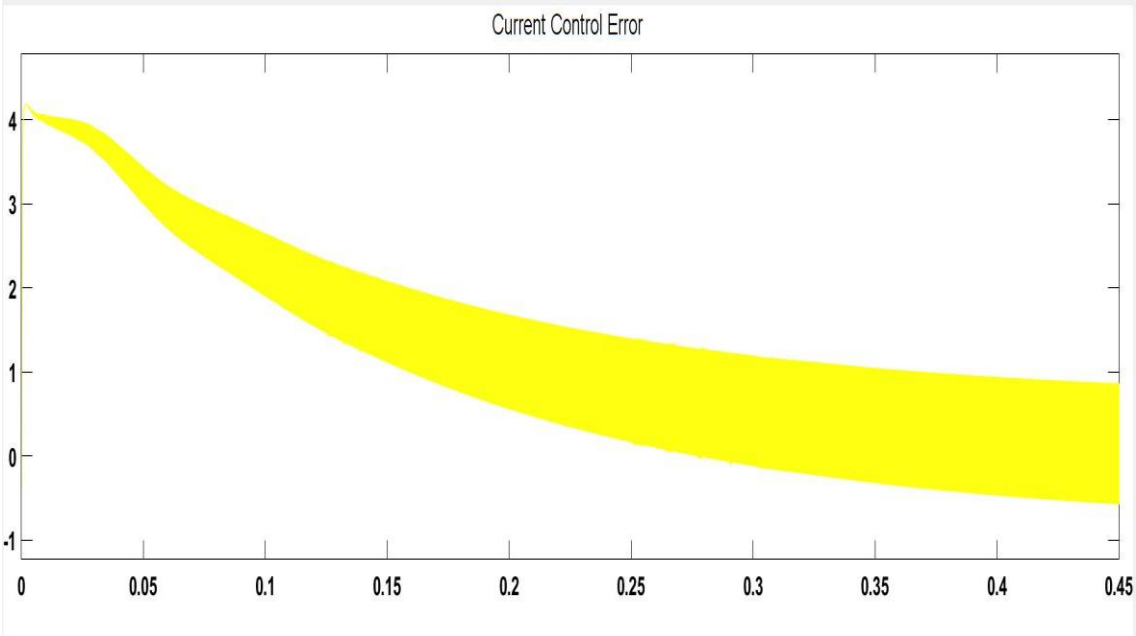

Fig. 23: PI control of the battery current

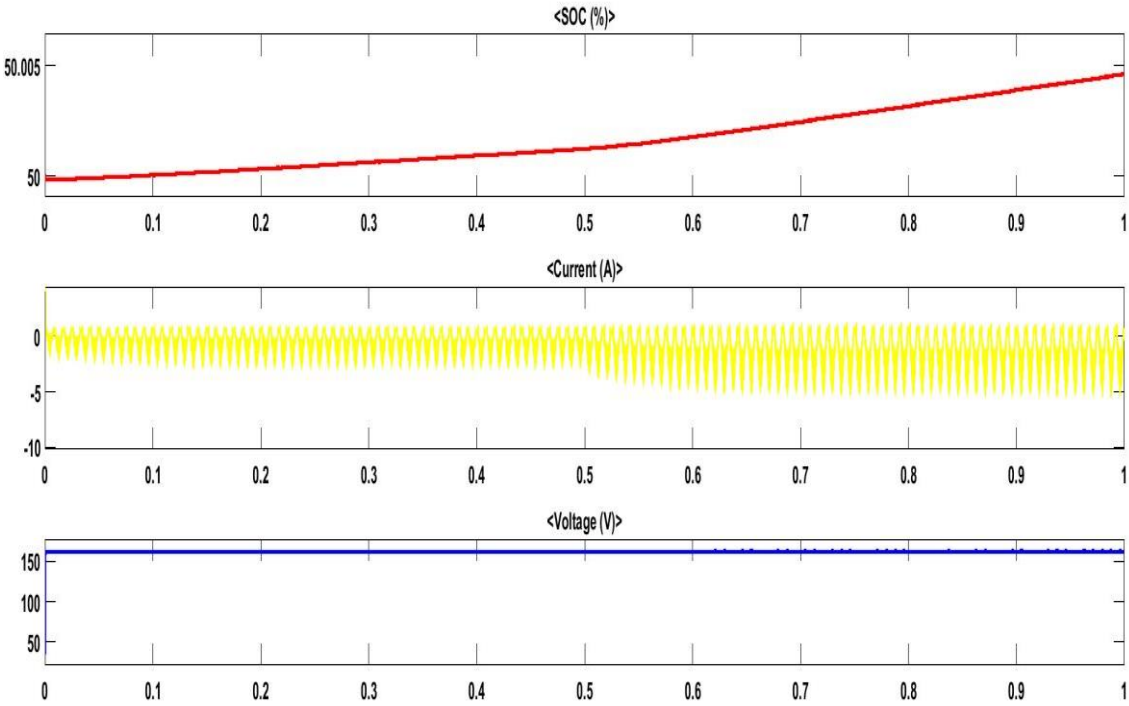

Fig. 24: Battery performance

4.3 THE MODEL PREDICTIVE CONTROLLED SYSTEM

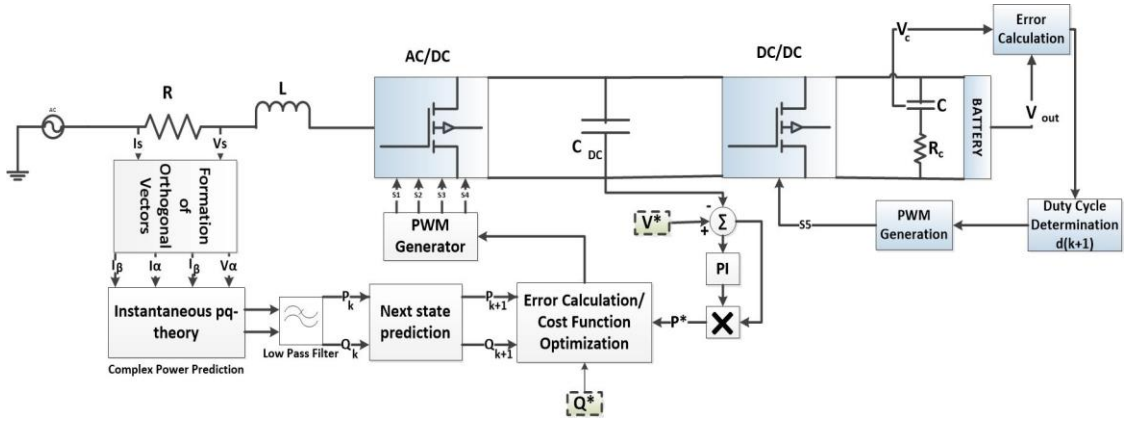

Fig. 25: Block Diagram of the MPC controlled charging system

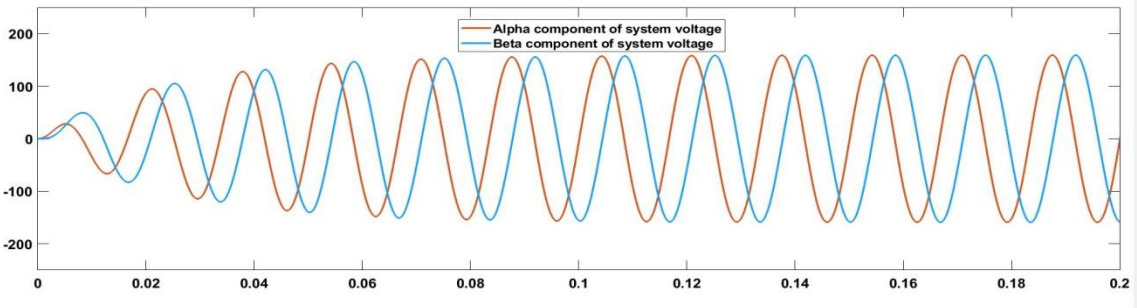

Fig. 26: Alpha-Beta components of the system voltage using SOGI

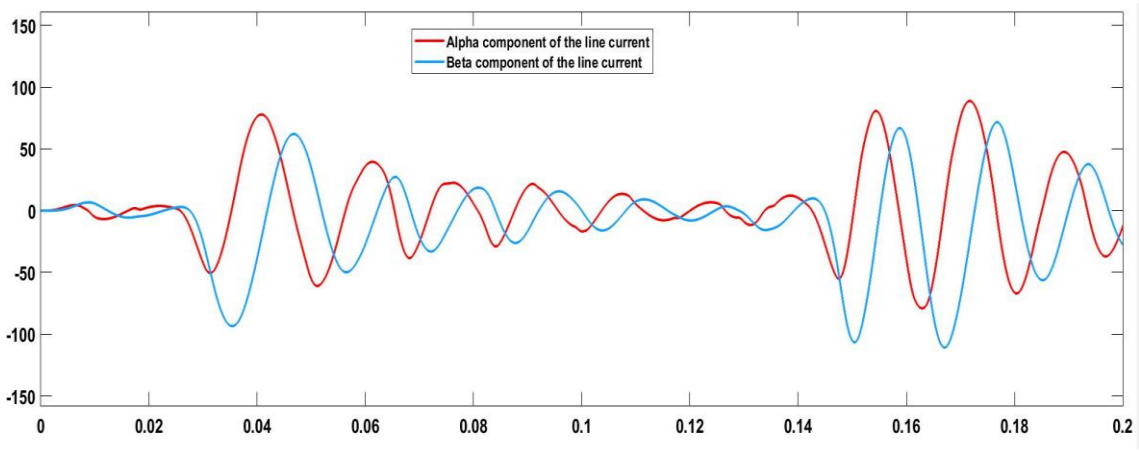

Fig. 27: Alpha Beta components of the source current using SOGI

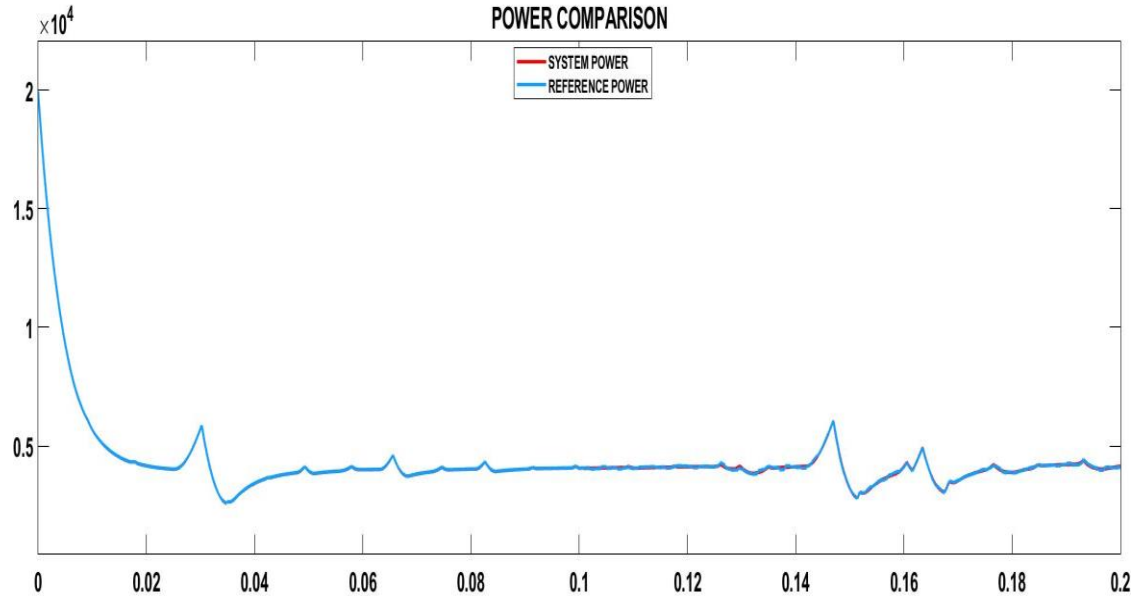

Fig. 28: Comparison of the Active Power controlled with the reference power generated

In the above figure, we can see that the output power of the system closely follows the reference power generated by the system and the overshoot has been eliminated completely.

Also, the settling time is in milliseconds which reflects the close tracking of power generated for reference, by the system.

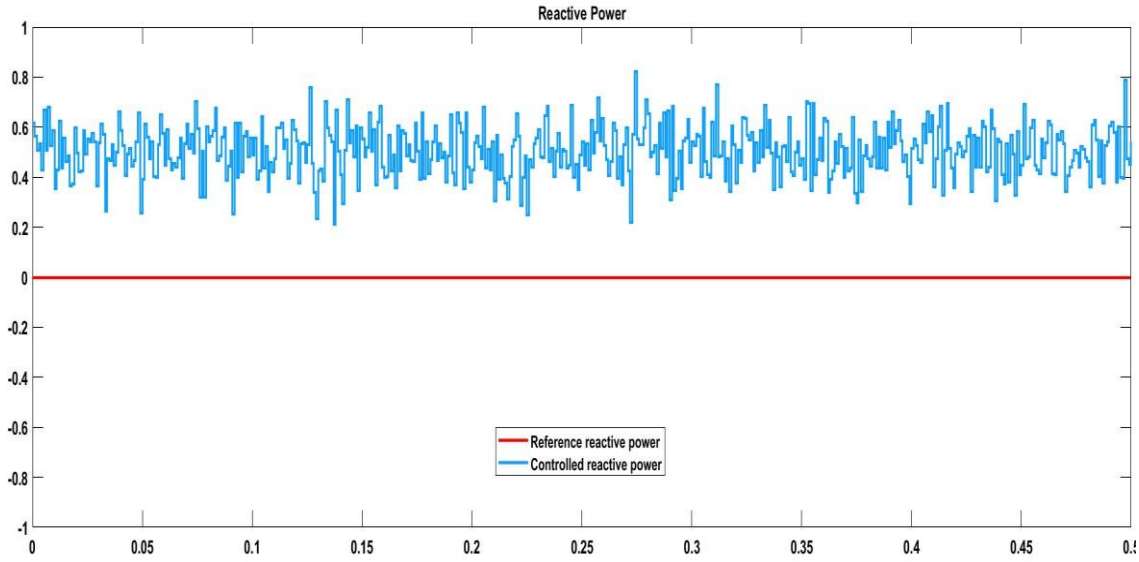

Fig. 29: Comparison of the Active Power controlled with the reference power generated

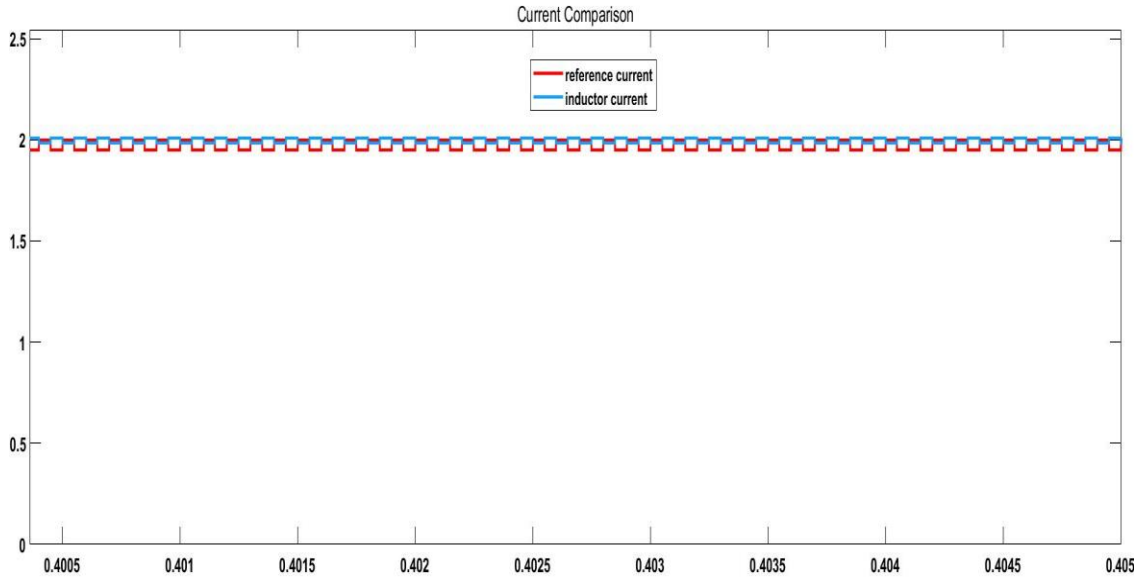

Fig. 30: MPC controlled inductor current comparison

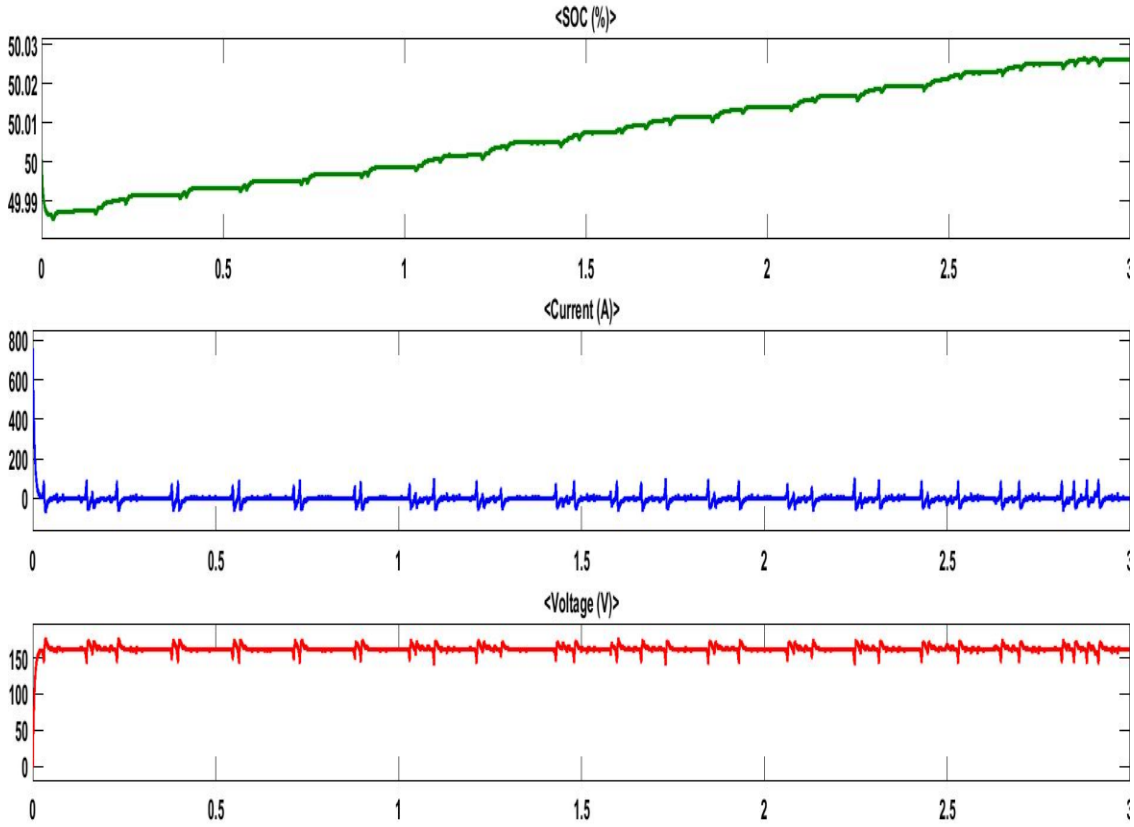

Fig. 31: MPC controlled battery characteristics

We can see that output of the MPC controlled system is far better than the PI controlled system.

CHAPTER 5

CONCLUSION AND FUTURE SCOPE

Proportional-Integral-Derivative and Model Predictive Control has been implemented separately in identical system or plants. Implementation of the conventional controlling gave a fair idea about the behavior of the system when performed under control. This helped in the way of implementation of the advanced controlling method.

When implementing the PI controlling, we can observe an overshoot in the output of the controlled active and reactive power, which settles after a certain time whenever any change is implemented in the reference signals. An immediate following of the reference signal by the controlled signal is desired in an ideal case, differing from which, in a practical scenario we can observe in the PI controlled case.

An improvement over this is observed when MPC is implemented in the place of PI in the plant. Here, we can see a better performance than the conventional control. There's a very small overshoot and deviation from the reference signal generated by the controller itself. Thereby, in MPC there is no need of manual controlling or changing of the reference. The reference is generated in accordance with the requirement of the system.

Few of the additional things that can be done in future is the implementation of charging for a battery pack i.e. when a number of batteries are in parallel and they get charged at the same rate and when the batteries are in series, they can be charged in a way such that there is no spilling of charge. Also the above controllers are implemented for a single phase system; they have the potential to be further extended to the three phases or two phase system. It can also be used to implement DC fast charging of the battery with less amount of heating.

REFERENCES

[1]. Murat Yilmaz, and Philip T. Krein, "Review of Battery Charger Topologies, Charging Power Levels, and Infrastructure for Plug-In Electric and Hybrid Vehicles", *IEEE transactions on power elec*., vol. 28, no. 5.

[2]. A. Ayob, W. M. F. W. Mahmood, A. Mohamed , M. Z. C Wanik, "Review on Electric Vehicle, Battery Charger, Charging Station and Standards", Research Journal of Applied Sciences, Engineering and Technology, ISSN: 2040-7459; e-ISSN: 2040-7467

[3]. Metin Kesler, Mithat C. Kisacikoglu, and Leon M. Tolbert, "Vehicle-to-Grid Reactive Power Operation Using Plug-In Electric Vehicle Bidirectional Off-board Charger", *IEEE transactions on industrial elec*., vol. 61, no. 12.

[4]. M. Forouzesh, Y. P. Siwakoti, Saman A. Gorji, Frede Blaabjerg, and Brad Lehman, "Step-Up DC–DC Converters: A Comprehensive Review of Voltage-Boosting Techniques, Topologies, and Applications", *IEEE transactions on power elec*., vol. 32, no. 12.

[5]. Mithat C. Kisacikoglu, M. Kesler, and Leon M. Tolbert, "Single-Phase On-Board Bidirectional PEV Charger for V2G Reactive Power Operation", *IEEE transactions on smart grid,* vol. 6, no. 2.

[6]. Sylvian L. Sanjaun, "Voltage Oriented Control of Three Phase PWM Boost Converters", *2010.*

[7]. A. I. Maswood, and F. Liu, "A Novel Variable Hysteresis Band Current Control of Three-Phase Three-Level Rectifier with Constant Switching Frequency," *IEEE Trans. Power Electron., vol. 21, no. 6, pp 1727 – 1734, November 2006*.

[8]. J. F. Bayona, H. R. Chamorro, A. C. Sanchez, J. A. Garcia, and D. A. Rubio, "Linear Control of a Power Factor Correction Rectifier in Half-bridge Configuration," *IEEE Trans. Power Electron., vol. 21, no. 6, pp 1727 - 1734, November 2006.*

[9]. B. Liu, Y. Zha, T. Zhang and S. Chen, "Sliding Mode Control for Rectifier stage of Solid State Transformer," *IEEE Trans. Power Electron., vol. 21, no. 6, pp 286 - 289, November 2016.*

[10]. Z. Leng and Q. Liu, “A Simple Model Predictive Control for Buck Converter operating in CCM,” *IEEE Trans. Power Electron., vol. 21, no. 6, pp 19 - 24, November 2017.*

[11]. A. Bouafia, F. Krim, and J. P. Gaubert, “Fuzzy-Logic-Based Switching State Selection for Direct Power Control of Three-Phase PWM Rectifier”, *IEEE Trans. on Industrial Electron., vol. 56, no. 6, June 2009.*

[12]. H. Bevrani, M. Abrishamchian, N. Safari-Shad, "Nonlinear and linear robust control of switching power converters", *Proceedings of the 1999 IEEE International Conference on Control Applications, vol. 1, pp. 808-813 vol. 1, August 1999.*

[13]. K. K. Monfared, H. Iman-Eini and R. Razi, "Control of Single-Phase Bidirectional PEV/EV Charger Based on FCS-MPC Method for V2G Reactive Power Operation," *2019 10th International Power Electronics, Drive Systems and Technologies Conference (PEDSTC), Shiraz, Iran, 2019, pp. 641-646, doi: 10.1109/PEDSTC.2019.8697783.*

[14]. M. P. Akter, S. Mekhilef, N. Tan and H. Akagi, ‘‘Modified model predictive control of a bidirectional ac-dc converter based on Lyapunov function for energy storage system,’’ in *IEEE Trans. Industrial Electron., vol. 63, no. 2, pp. 704-715, Feb. 2016.*

[15]. S. Kouro, P. Cortes, R. Vargas, U. Ammann and J. Rodriguez, ‘‘Model predictive control-a simple and powerful method to control power converters,’’ in *IEEE Trans. Industrial Electron., vol. 56, no. 6, pp. 1826-1838, Jun. 2009.*

[16]. M. Parvez, S. Mekhilef, N. Tan and H. Akagi, ‘‘Model predictive control of a bidirectional ac-dc converter for V2G and G2V applications in electric vehicle battery charger,’’ in *Transportation Electrification Conference and Expo (ITEC), pp. 1-6, Jun. 2014.*

[17]. E. Jun, S. Kwak and T. Kim, "Performance Comparison of Model Predictive Control Methods for Active Front End Rectifiers," *in IEEE Access, vol. 6, pp. 77272-77288, 2018, doi: 10.1109/ACCESS.2018.2881133*.

[18]. S. Vazquez, J. A. Sanchez, J. M. Carrasco, J. I. Leon and E. Galvan, "A Model-Based Direct Power Control for Three-Phase Power Converters," *in IEEE Transactions on Industrial Electronics, vol. 55, no. 4, pp. 1647-1657, April 2008, doi: 10.1109/TIE.2008.917113.*

[19]. J. Sebastian, A. Fernandez, P. J. Villegas, M. M. Hernando and J. M. Lopera, "Improved active input current shapers for converters with symmetrically driven transformer," *in IEEE Transactions on Industry Applications, vol. 37, no. 2, pp. 592-600, March-April 2001, doi: 10.1109/28.913726.*

[20]. E. Mudaheranwa, A. Rwigema, E. Ntagwirumugara, G. Masengo, R. Singh and J. Biziyaremye, "Development of PLC based monitoring and control of pressure in Biogas Power Plant Digester," *2019 International Conference on Advances in Big Data, Computing and Data Communication Systems (icABCD), Winterton, South Africa, 2019, pp. 1-7, doi: 10.1109/ICABCD.2019.8851046.*

[21]. J. Hu, L. Shang, Y. He and Z. Q. Zhu, "Direct Active and Reactive Power Regulation of Grid-Connected DC/AC Converters Using Sliding Mode Control Approach," *in IEEE Transactions on Power Electronics, vol. 26, no. 1, pp. 210-222, Jan. 2011, doi: 10.1109/TPEL.2010.2057518.*

[22]. Prasoon C. Mavila, and Nisha B. Kumar, "A bi-directional dc-dc battery interface for EV charger with G2V and V2X capability", *International Journal of Innovative Research in Science, Engineering and Technology, Vol. 5, Special Issue 5, April 2016.*

[23]. J. Gupta and B. Singh, "A Bidirectional Home Charging Solution for an Electric Vehicle," *2019 IEEE International Conference on Environment and Electrical Engineering and 2019 IEEE Industrial and Commercial Power Systems Europe, pp. 1-6, August 2019.*

[24]. Lie Xu, Da W. Zhi, and Liang Z. Yao, "Direct Power Control of Grid Connected Voltage Source Converters".

[25]. Dong-Eok Kim and Dong-Choon Lee, "Feedback linearization control of three-phase AC/DC PWM converters with LCL input filters," *2007 7th Internatonal Conference on Power Electronics, Daegu, 2007, pp. 766-771, doi: 10.1109/ICPE.2007.4692491.*

[26]. N. Saxena, I. Hussain, B. Singh, and A. L. Vyas, "Implementation of a Grid Integrated PV-Battery System for Residential and Electrical Vehicle Applications", *IEEE Transactions on Industrial Electronics, vol. 65, no. 8, August 2018.*

[27]. T. He, J. Zhu, D. Lu, and L. Zheng, "Modified Model Predictive Control for Bidirectional Four-Quadrant EV Chargers With Extended Set of Voltage Vectors", *IEEE Journal of Emerging and Selected Topics in Power Electron., vol. 7, no. 1, March 2019.*

[28]. M. Falahi, Hung-Ming Chou, M. Ehsani, L. Xie, and K. L. Butler-Purry, " Potential Power Quality Benefits of Electric Vehicles", *IEEE Transactions on Sustainable Energy, vol. 4, no. 4, October 2013.*

[29]. I. Cvetkovic, T. Thacker, D. Dong, G. Francis, V. Podosinov, and D. Boroyevich *et al.*, "Future home uninterruptable renewable energy system with vehicle-to-grid technology," in *Proc. Energy Convers. Congr. Expos.*, 2009, pp. 2675–2681.

[30]. A. G. Boulanger, A. C. Chu, S. Maxx, and D. L.Waltz, "Vehicle electrification: Status and issues," *Proc. IEEE, vol. 99, no. 6, pp. 1116–1138, June 2011.*

[31]. M. C. Kisacikoglu, "Vehicle-to-Grid (V2G) reactive power operation analysis of the EV/PHEV bidirectional battery charger," *Univ. Tennessee, Knoxville, TN, USA, May 2013.*

[32]. M. Yilmaz and P. T. Krein, "Review of the impact of vehicle-to-grid technologies on distribution systems and utility interfaces," *IEEE Trans. Power Electron., vol. 28, no. 12, pp. 5573–5689, December 2013.*

[33]. M. H. Rashid, *Power Electronics Handbook: Devices Circuits and Application*, 3rd ed. Burlington, MA, USA: Elsevier, 2011.

[34]. M. K. Kazimierczuk, D. Q. Vuong, B. T. Nguyen, and J. A. Weimer, "Topologies of bidirectional PWM DC-DC power converters," in *Proc. IEEE Nat. Aerosp. Electron. Conf., 1993, pp. 435–441.*

[35]. H. Fakham, D. Lu, and B. Francois, "Power control design of a battery charger in a hybrid active PV generator for load-following applications," *IEEE Trans. Ind. Electron., vol. 58, no. 1, pp. 85–94, Jan. 2011.*

[36]. M. C. Kisacikoglu, B. Ozpineci, and L. M. Tolbert, "EV/PHEV bidirectional charger assessment for V2G reactive power operation," *IEEE Trans. Power Electron., vol. 28, no. 12, pp. 5717–5727, Dec. 2013.*

[37]. Y. Zhang, W. Xie, Z. Li, and Yingchao Zhang, " Low Complexity Model Predictive Control: Double Vector Based Approach", *IEEE Transactions on Industrial Electronics, vol. 61, no. 11, November 2014.*

[38]. J. G. Pinto, V. Monteiro, H. Goncalves, and J. L. Afonso, "On-board reconfigurable battery charger for electric vehicles with traction-to-auxiliary model," *IEEE Trans. Veh. Technol., vol. 63, no. 3, pp. 1104–1116, Mar. 2014.*

[39]. Z. Song, W. Chen, and C. Xia, “Predictive direct power control for three-phase grid-connected converters without sector information and voltage vector selection,” *IEEE Trans. Power Electron., vol. 29, no. 10, pp. 5518–5531, Oct. 2014.*

[40]. J. R. Fischer, S. A. Gonzlez, I. Carugati, M. A. Herran, M. G. Judewicz, and D. O. Carrica, “Robust predictive control of grid-tied converters based on direct power control,” *IEEE Trans. Power Electron., vol. 29, no. 10, pp. 5634–5643, Oct. 2014.*

[41]. Y. Zhang, Z. Li, Y. Zhang, W. Xie, Z Piao, and C Hu, “Performance improvement of direct power control of PWM rectifier with simple calculation,” *IEEE Trans. Power Electron., vol. 28, no. 7, pp. 3428–3437, July 2013.*

[42]. K. G. Pavlou, M. Vasiladiotis, and S. N. Manias, “Constrained model predictive control strategy for single-phase switch-mode rectifiers,” *IET Power Electron., vol. 5, no. 1, pp. 31–40, Jan. 2012.*

[43]. Liuping Wang, “ Model Predictive Control, Design and Implementation using MATLAB”, *2009 Springer-Verlag London Limited.*

[44]. J. Rodriguez and P. Cortes, “ Predictive Control of Power Converters and Electrical Drives”, *2012, John Wiley & Sons, Ltd.*

[45]. X. Guo, Hai-Peng Ren, and J. Li, “Robust Model-Predictive Control for a Compound Active-Clamp Three-Phase Soft-Switching PFC Converter Under Unbalanced Grid Condition”, *IEEE Transactions on Industrial Electronics, vol. 65, no. 3, March 2018.*

[46]. S. Jain, M. Easley, M. B. Shadmand and B. Mirafzal, "Decoupled active and reactive power predictive control of impedance source microinverter with LVRT capability," *2018 IEEE Power and Energy Conference at Illinois (PECI), Champaign, IL, 2018, pp. 1-6, doi: 10.1109/PECI.2018.8334982.*

[47]. M. Ciobotaru, R. Teodorescu and F. Blaabjerg, "A new single-phase PLL structure based on second order generalized integrator," *2006 37th IEEE Power Electronics Specialists Conference, Jeju, 2006, pp. 1-6, doi: 10.1109/pesc.2006.1711988.*

[48]. R. Li, and D. Xu, “A Zero-Voltage Switching Three-Phase Inverter”, *IEEE Transactions on Power Electronics, vol. 29, no. 3, March 2014.*

[49]. R. Teodorescu, F. Blaabjerg, M. Liserre, and P. Loh, “Proportional-resonant controllers and filters for grid-connected voltage-source converters,” *IEE Proc. Elect. Power Appl., vol. 153, no. 5, pp. 750–762, September 2006.*

[50]. B. Delfino and F. Fornari, "Modeling and control of an integrated fuel cell-wind turbine system," *2003 IEEE Bologna Power Tech Conference Proceedings,, Bologna, Italy, 2003, pp. 6 pp. Vol.2-, doi: 10.1109/PTC.2003.1304613.*

[51]. https://enertechint.com

[52]. en.wikipedia.org

[53]. T. He, J. Zhu, D. D. Lu and L. Zheng, "Modified Model Predictive Control for Bidirectional Four-Quadrant EV Chargers With Extended Set of Voltage Vectors," *in IEEE Journal of Emerging and Selected Topics in Power Electronics, vol. 7, no. 1, pp. 274-281, March 2019, doi: 10.1109/JESTPE.2018.2870481.*

[54]. M. Yilmaz and P. T. Krein, "Review of charging power levels and infrastructure for plug-in electric and hybrid vehicles," *2012 IEEE International Electric Vehicle Conference, Greenville, SC, 2012, pp. 1-8, doi: 10.1109/IEVC.2012.6183208.*

[55]. electricvehicle.ieee.org

[56]. Dong-Jing Lee and Li Wang, "Control of autonomous solid oxide fuel cells subject to sudden load variations," *2008 IEEE/PES Transmission and Distribution Conference and Exposition, Chicago, IL, 2008, pp. 1-5, doi: 10.1109/TDC.2008.4517298.*